Mobile Assemblies of Four-Spherical-4R-integrated Linkages and the Associated Four-crease-integrated Rigid Origami Patterns

Yan Chen[a], Weilin Lv[a], Rui Peng[a], and Guowu Wei[b,*]

a) School of Mechanical Engineering, Tianjin University, Tianjin 300350, China
b) School of Science, Engineering and Environment, University of Salford, Salford M5 4WT, UK

Abstract

Rigid origami, which can be regarded as assemblies of spherical linkages, inspires a new paradigm of design for mechanical metamaterials and deployable structural systems with large deployable ratio. In this paper, the kinematic properties of assemblies of spherical 4R linkages are studied, and new origami patterns are obtained. Kinematics of a single loop spherical 4R linkage is firstly presented, and by assigning four specified values for the four twist angles, and defining four pairs of specified input and output angles, 16 maps between the input and output angles are obtained together with 256 types of special spherical 4R linkages. By merging four identical spherical 4R linkages into a single loop, three basic mobile assemblies are constructed and the one-degree-of-freedom kinematic compatibility condition is formulated. Through alteration of the four vertex linkages in the three basic assemblies, variations of the basic assemblies are generated. Consequently, by adding further geometric conditions, novel rigid origami patterns are obtained leading to the tessellation of the spherical-4R-linkage-integrated assemblies. Hence, this paper provides a novel approach for generating new rigid origami patterns which can lead to the development of foldable structures and tessellations with potential applications in robotics, smart architectures, and space exploration.

Keywords: spherical 4R linkage; kinematic compatibility; mobile assembly; rigid origami; tessellation

1. Introduction

Origami is a traditional art and it is a continuous, one-to-one mapping of a crease pattern to create a three-dimensional object. Rigid origami, which is referred to the case that each paper facet surrounded with creases is not stretching or bending during folding. Because of the large deployable ratio and low cost, rigid origami patterns have significant potentials in various applications such as robotic systems [1, 2], deployable arrays for space applications [3], and self-deploy structures [4].

*Corresponding author

Emails: yan.chen@tju.edu.cn (Y. Chen), lvweilin@tju.edu.cn (W. Lv), pengrui@tju.edu.cn (R. Peng), g.wei@salford.ac.uk (G.Wei)

On the one hand, rigid origami has been investigated from the viewpoint of geometry. Miura [5] presented a proposition of intrinsic geometry of origami based on an arbitrary point on the surface of origami works. Watanabe and Kawaguchi [6] proposed two methods to judging rigid foldability of origami patters from the compatibility matrix. Based on separating each crease of an origami pattern into two parallel creases, Hull and Tachi [7] presented the double line method to obtain new origami patterns. And recently, He and Guest [8] studied the configuration space of four-crease origami patterns and generated two families of rigid-foldable origami patterns with four-crease vertexes.

On the other hand, rigid origami can be studied with a kinematic approach, where its facets and crease lines can be replaced by rigid panels and hinges [9]. In particular, a four-crease vertex can be represented by a spherical 4R linkage [10-12]. Wu and You [13] proposed a new crease pattern that allows a tall box-shaped bag with a rectangular base to be rigidly folded flat. The typical origami crease patterns and their corresponding equivalent closed-loop linkage were investigated by Zhang and Dai [14]. Wei and Dai [15] analyzed an origami carton by representing it with one planar four-bar loop and two spherical 4R linkage loops. With the tessellation method for mobile assemblies of spatial linkages [16-18], Wang and Chen [19] proposed the mobile assembly [20] of spherical 4R linkages to study the Kokotsakis type of the rigid origami patterns. Liu [21] used the assemblies of spherical 4R linkages to analyze the rigid origami patterns and presented several new patterns. Based on the kinematics of spherical 4R linkages, Liu et al. [22] presented several types of rigid origami tubes, and recently Chen et al. [23] proposed an extended family of them. However, the spherical 4R linkage method applied to analyze rigid origami patterns requests quite complicated closure equations, which limits the design of rigid origami. This prompted us to think whether 4R linkage method could be improved.

In this paper, a new method for synthesizing novel rigid origami patterns is proposed. The approach is based on the development a family of mobile assemblies with spherical 4R linkage of various formats and thus forming the corresponding rigid origami patterns. Kinematics of spherical 4R linkage is presented and 1-DOF mobile assemblies formed by four spherical 4R linkages are developed. Then based the equivalence between linkage and rigid origami, innovative design of rigid origami patterns is proposed demonstrated by the generation of a helical pattern rigid origami.

2. Kinematics of a Spherical 4R Linkage and Maps between Special Input and Output Angles

Origami is seen in different forms in our daily life, and since the research by Cundy [24] it is widely acknowledged that for every rigid origami there correspondingly exists an equivalent linkage [9, 25]. Figure 1(a) shows a degree-4 origami vertex containing four panels or sectors 1 to 4, and four creases A, B, C and D; the four creases intersect at a common point O. The four sector angles between the adjacent creases are α_{12}, α_{23}, α_{34} and α_{41}; and the four dihedral angles between the adjacent sectors are θ_1, θ_2, θ_3, and θ_4. From the mechanism point of view, by taking the sectors as links and the creases as revolute joints, an equivalent spherical 4R linkage can be obtained in Fig. 1(b); where sectors 1 to 4 become links 1 to 4, creases A to D become joints A_1 to A_4, and sector angels α_{12}, α_{23}, α_{34} and α_{41} become twist angles of the linkage. Hence, kinematics for the spherical 4R linkage can be applied to the kinematic analysis of the degree-4 origami vertex [26].

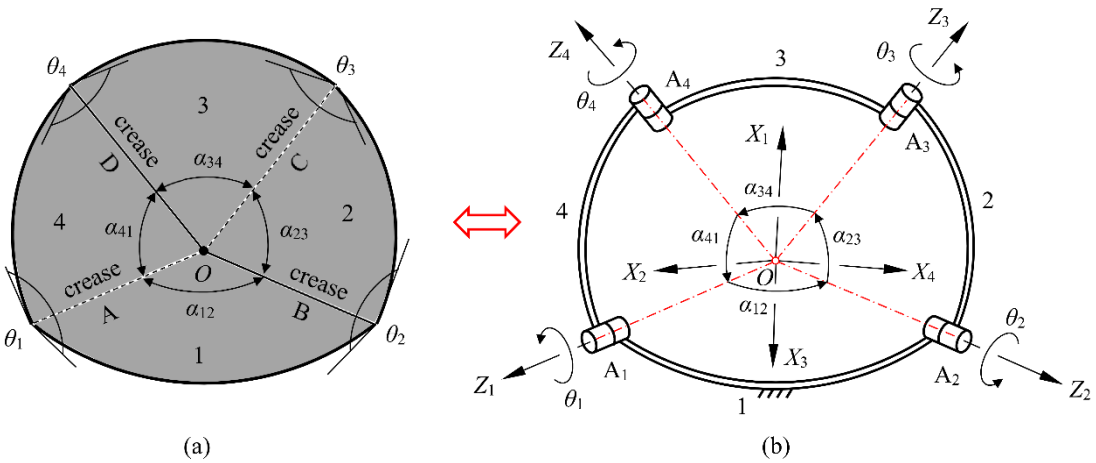

Figure 1 A degree-4 origami vertex and its equivalent spherical 4R linkage

In Fig. 1(b), by following the D-H convention [27], coordinate frames $\mathcal{F}_i$ are established at the joints of the linkage. Where, the Z_i-axis (i = 1, 2, 3 and 4) is along the joint axis of joint A_i; X_i-axis is normal to the plane formed by the Z_i and Z_{i+1} axes such that $X_i = Z_i \times Z_{i+1}$ (it should be noted that when the subscript $i + 1 = 5$, it is replaced with 1); Y_i-axis can be found with right-hand rule and the origin O_i of each coordinate frame coincides with point O. Angle θ_{i+1} is defined as joint angle from the X_i-axis to the X_{i+1}-axis, positively about Z_{i+1}-axis; and angle $\alpha_{i(i+1)}$ is the twist angle from Z_i to Z_{i+1} positively about axis X_i (when $i + 1 = 5$, it is replaced with 1). Further, link length $a_{i(i+1)}$ is defined as the distance of the common perpendicular between Z_i and Z_{i+1} along X_i, and offset d_{i+1} is defined as the distance between X_i to X_{i+1} along Z_{i+1}. For the spherical 4R linkage, since all the four revolute joints intersect at a common point O, it has $a_{12} = a_{23} = a_{34} = a_{41} = 0$, and $d_1 = d_2 = d_3 = d_4 = 0$ such that there is no translation between the coordinate frames.

Treating two adjacent joint angels θ_i, θ_{i+1} one, e.g. θ_i as input and the other one, i.e. θ_{i+1} as output, based on the loop equation that $\mathbf{R}_{12}\mathbf{R}_{23}\mathbf{R}_{34}\mathbf{R}_{41} = \mathbf{I}$ with $\mathbf{R}_{ij}$ being the rotation matrix and I being a 3 × 3 identity matrix, the general relationship between two adjacent joint angles can be given as

$$\begin{aligned}
&\sin\alpha_{i(i+1)}\cos\alpha_{(i+1)(i+2)}\sin\alpha_{(i+3)(i+4)}\cos\theta_i \\
&+\sin\alpha_{i(i+1)}\sin\alpha_{(i+1)(i+2)}\cos\alpha_{(i+3)(i+4)}\cos\theta_{i+1} \\
&+\cos\alpha_{i(i+1)}\sin\alpha_{(i+1)(i+2)}\sin\alpha_{(i+3)(i+4)}\cos\theta_i\cos\theta_{i+1} \\
&-\sin\alpha_{(i+1)(i+2)}\sin\alpha_{(i+3)(i+4)}\sin\theta_i\sin\theta_{i+1} \\
&-\cos\alpha_{i(i+1)}\cos\alpha_{(i+1)(i+2)}\cos\alpha_{(i+3)(i+4)}+\cos\alpha_{(i+2)(i+3)}=0
\end{aligned} \tag{1}$$

And the detailed derivation of Eq. (1) can be found in [28]. In the Eq. (1), subscript i is the number of stating joint and subscript $i + j$ (j = 1, 2, 3, 4) is the number for the sequential joint. In the case that $i + j > 4$, with i = 1, 2, 3 and 4, and j = 1, 2, 3 and 4, $i + j$ needs to be replaced by $i + j – 4$. For example, referring to Fig. 1 in the paper, the spherical 4R linkage has just four twist angles, if the stating joint i = 3 then the twist angle between joint $i + 1$ and $i + 2$ (with j = 1 and 2) becomes $\alpha_{(i+1)(i+2)}$, i.e. α_{45}, which

does not exist and the actual twist angle should be α_{41}; in which $i + 2 = 3 + 2 = 5 > 4$ is replaced by $i + 2 - 1 = 3 + 2 - 1 = 1$.

Solving the trigonometric equation in Eq. (1) leads to

$$\theta_{i+1} = \pm\cos^{-1}\left(\frac{k_3}{\sqrt{k_1^2 + k_2^2}}\right) - \tan^{-1}\frac{k_2}{k_1} \tag{2}$$

With $k_1 = \sin\alpha_{i(i+1)}\sin\alpha_{(i+1)(i+2)}\cos\alpha_{(i+3)(i+4)} + \cos\alpha_{i(i+1)}\sin\alpha_{(i+1)(i+2)}\sin\alpha_{(i+3)(i+4)}\cos\theta_i$, $k_2 = \sin\alpha_{(i+2)(i+3)}\sin\alpha_{(i+3)(i+4)}\sin\theta_i$ and $k_3 = \cos\alpha_{i(i+1)}\cos\alpha_{(i+1)(i+2)}\cos\alpha_{(i+3)(i+4)} - \cos\alpha_{(i+2)(i+3)} - \sin\alpha_{i(i+1)}\cos\alpha_{(i+1)(i+2)}\sin\alpha_{(i+3)(i+4)}\cos\theta_i$, all being the functions of θ_i.

Equation (2) gives the explicit function between the output angle θ_{i+1} and the input angle θ_i which can also be represented concisely in implicit function form as

$$\theta_{i+1} = f_{i(i+1)}(\theta_i) \tag{3}$$

Further, by substituting $-\theta_i$ and $-\theta_{i+1}$ into Eq. (1), due to the relations that $\cos(-\theta_i) = \cos\theta_i$, $\cos(-\theta_{i+1}) = \cos\theta_{i+1}$, $\cos\theta_i\cos\theta_{i+1} = \cos(-\theta_i)\cos(-\theta_{i+1})$, and $\sin\theta_i\sin\theta_{i+1} = \sin(-\theta_i)\sin(-\theta_{i+1})$, it is found that all the five terms on the left hand side of Eq. (1) remain unchanged, hence there exists the following relation:

$$-\theta_{i+1} = f_{i(i+1)}(-\theta_i) = -f_{i(i+1)}(\theta_i) \tag{4}$$

which implies that a minus input results in a minus output.

In this paper, it is interesting to find that by altering the twist angles $\alpha_{(i+j)(i+j+1)}$ into four cases as $\alpha_{(i+j)(i+j+1)}$, $-\alpha_{(i+j)(i+j+1)}$, $\pi - \alpha_{(i+j)(i+j+1)}$, and $-\pi + \alpha_{(i+j)(i+j+1)}$, there exist different maps between the special input and output angles of the spherical 4R linkage such that given the input as either of the four values as θ_i, $\pi - \theta_i$, $-\pi + \theta_i$, or $-\theta_i$, each can lead to four results for the output angle as θ_{i+1}, $\pi - \theta_{i+1}$, $-\pi + \theta_{i+1}$, or $-\theta_{i+1}$. For each of the case, by taking the map from θ_i to $-\theta_{i+1}$, that is denoted as m_4 in this paper, as an example, there are 16 different combinations of the four twist angles $\alpha_{(i+j)(i+j+1)}$, $-\alpha_{(i+j)(i+j+1)}$, $\pi - \alpha_{(i+j)(i+j+1)}$, and $-\pi + \alpha_{(i+j)(i+j+1)}$ that can lead to the same map based on Eq. (1); and these 16 combinations provide 16 variations of the spherical 4R linkage as listed in Table 1.

Table 1 Map m_4, the associated combinations of twist angles and variations of spherical 4R linkage

Map	Combinations of $\alpha_{(i+j)(i+j+1)}$, $-\alpha_{(i+j)(i+j+1)}$, $\pi - \alpha_{(i+j)(i+j+1)}$, and $-\pi + \alpha_{(i+j)(i+j+1)}$	Variations f_{ij}
m_4: $\theta_i \rightarrow -\theta_{i+1}$	$\pi - \alpha_{i(i+1)}$, $\pi - \alpha_{(i+1)(i+2)}$, $\alpha_{(i+2)(i+3)}$, $-\alpha_{(i+3)(i+4)}$	v_{41}: m_4-c_1
	$\pi - \alpha_{i(i+1)}$, $\pi - \alpha_{(i+1)(i+2)}$, $\pi - \alpha_{(i+2)(i+3)}$, $\pi - \alpha_{(i+3)(i+4)}$	v_{42}: m_4-c_2
	$\pi - \alpha_{i(i+1)}$, $\pi - \alpha_{(i+1)(i+2)}$, $-\pi + \alpha_{(i+2)(i+3)}$, $\pi - \alpha_{(i+3)(i+4)}$	v_{43}: m_4-c_3

	$\pi - \alpha_{i(i+1)}$, $\pi - \alpha_{(i+1)(i+2)}$, $-\alpha_{(i+2)(i+3)}$, $- \alpha_{(i+3)(i+4)}$	v_{44}: m_4-c_4
	$\pi - \alpha_{i(i+1)}$, $- \alpha_{(i+1)(i+2)}$, $\alpha_{(i+2)(i+3)}$, $\pi - \alpha_{(i+3)(i+4)}$	v_{45}: m_4-c_5
	$\pi - \alpha_{i(i+1)}$, $- \alpha_{(i+1)(i+2)}$, $\pi - \alpha_{(i+2)(i+3)}$, $- \alpha_{(i+3)(i+4)}$	v_{46}: m_4-c_6
	$\pi - \alpha_{i(i+1)}$, $- \alpha_{(i+1)(i+2)}$, $- \pi + \alpha_{(i+2)(i+3)}$, $- \alpha_{(i+3)(i+4)}$	v_{47}: m_4-c_7
	$\pi - \alpha_{i(i+1)}$, $- \alpha_{(i+1)(i+2)}$, $- \alpha_{(i+2)(i+3)}$, $\pi - \alpha_{(i+3)(i+4)}$	v_{48}: m_4-c_8
	$-\pi + \alpha_{i(i+1)}$, $\alpha_{(i+1)(i+2)}$, $\alpha_{(i+2)(i+3)}$, $-\pi + \alpha_{(i+3)(i+4)}$	v_{49}: m_4-c_9
	$-\pi + \alpha_{i(i+1)}$, $\alpha_{(i+1)(i+2)}$, $\pi + \alpha_{(i+2)(i+3)}$, $\alpha_{(i+3)(i+4)}$	v_{410}: m_4-c_{10}
	$-\pi + \alpha_{i(i+1)}$, $\alpha_{(i+1)(i+2)}$, $-\pi + \alpha_{(i+2)(i+3)}$, $\alpha_{(i+3)(i+4)}$	v_{411}: m_4-c_{11}
	$-\pi + \alpha_{i(i+1)}$, $\alpha_{(i+1)(i+2)}$, $-\alpha_{(i+2)(i+3)}$, $-\pi + \alpha_{(i+3)(i+4)}$	v_{412}: m_4-c_{12}
	$-\pi + \alpha_{i(i+1)}$, $-\pi + \alpha_{(i+1)(i+2)}$, $\alpha_{(i+2)(i+3)}$, $\alpha_{(i+3)(i+4)}$	v_{413}: m_4-c_{13}
	$-\pi + \alpha_{i(i+1)}$, $-\pi + \alpha_{(i+1)(i+2)}$, $\pi - \alpha_{(i+2)(i+3)}$, $-\pi + \alpha_{(i+3)(i+4)}$	v_{414}: m_4-c_{14}
	$-\pi + \alpha_{i(i+1)}$, $-\pi + \alpha_{(i+1)(i+2)}$, $\pi + \alpha_{(i+2)(i+3)}$, $-\pi + \alpha_{(i+3)(i+4)}$	v_{415}: m_4-c_{15}
	$-\pi + \alpha_{i(i+1)}$, $-\pi + \alpha_{(i+1)(i+2)}$, $- \alpha_{(i+2)(i+3)}$, $\alpha_{(i+3)(i+4)}$	v_{416}: m_4-c_{16}

In Table 1, m_4 stands for the 4th map and c_i (i = 1 to 16) denotes the ith combination; hence, map m_4 contains 16 different types of variations of spherical 4R linkage that can lead to the same map that can achieve $-\theta_{i+1}$ by given an adjacent input angle θ_i. It should be pointed out that due to the combination of the twist angles, the 16 variations of Map m_4 listed in Table 1 are not always different. Nevertheless, it is found that for each variation v_{4i} in map m_4, there always exists at least one variation v_{4j} which is identical with it in the case that $\alpha_{i(i+1)}$ is related to $\alpha_{(i+3)(i+4)}$ with π, $-\pi$ or inverse.

Further, from the specified input angles θ_i, $\pi - \theta_i$, $-\pi + \theta_i$, and $-\theta_i$ to the specified output angles θ_{i+1}, $\pi - \theta_{i+1}$, $-\pi + \theta_{i+1}$, or $-\theta_{i+1}$, there are totally 16 maps which are listed in Table 2.

Table 2 Maps between the special input and output angles

Map i	Relationship between the input and output angles
m_1	$\theta_i \longrightarrow \theta_{i+1}$: $\{\theta_{i+1} = f_{i(i+1)}(\theta_i)\}$
m_2	$\theta_i \longrightarrow \pi - \theta_{i+1}$: $\{\pi - \theta_{i+1} = f_{i(i+1)}(\theta_i)\}$
m_3	$\theta_i \longrightarrow - \pi + \theta_{i+1}$: $\{- \pi + \theta_{i+1} = f_{i(i+1)}(\theta_i)\}$
m_4	$\theta_i \longrightarrow - \theta_{i+1}$: $\{- \theta_{i+1} = f_{i(i+1)}(\theta_i)\}$
m_5	$\pi - \theta_i \longrightarrow \theta_{i+1}$: $\{\theta_{i+1} = f_{i(i+1)}(\pi - \theta_i)\}$
m_6	$\pi - \theta_i \longrightarrow \pi - \theta_{i+1}$: $\{\pi - \theta_{i+1} = f_{i(i+1)}(\pi - \theta_i)\}$
m_7	$\pi - \theta_i \longrightarrow - \pi + \theta_{i+1}$: $\{- \pi + \theta_{i+1} = f_{i(i+1)}(\pi - \theta_i)\}$
m_8	$\pi - \theta_i \longrightarrow - \theta_{i+1}$: $\{- \theta_{i+1} = f_{i(i+1)}(\pi - \theta_i)\}$

m_9	$-\theta_i \rightarrow -\theta_{i+1}$: $\{-\theta_{i+1} = f_{i(i+1)}(-\theta_i)\}$
m_{10}	$-\theta_i \rightarrow -\pi + \theta_{i+1}$: $\{-\pi + \theta_{i+1} = f_{i(i+1)}(-\theta_i)\}$
m_{11}	$-\theta_i \rightarrow \pi - \theta_{i+1}$: $\{\pi - \theta_{i+1} = f_{i(i+1)}(-\theta_i)\}$
m_{12}	$-\theta_i \rightarrow \theta_{i+1}$: $\{\theta_{i+1} = f_{i(i+1)}(-\theta_i)\}$
m_{13}	$-\pi + \theta_i \rightarrow -\theta_{i+1}$: $\{-\theta_{i+1} = f_{i(i+1)}(-\pi + \theta_i)\}$
m_{14}	$-\pi + \theta_i \rightarrow -\pi + \theta_{i+1}$: $\{-\pi + \theta_{i+1} = f_{i(i+1)}(-\pi + \theta_i)\}$
m_{15}	$-\pi + \theta_i \rightarrow \pi - \theta_{i+1}$: $\{\pi - \theta_{i+1} = f_{i(i+1)}(-\pi + \theta_i)\}$
m_{16}	$-\pi + \theta_i \rightarrow \theta_{i+1}$: $\{\theta_{i+1} = f_{i(i+1)}(-\pi + \theta_i)\}$

Where in Table 2, $f_{i(i+1)}(\theta)$ is the function obtained in Eq. (3). Since there exists $-\theta_{i(i+1)} = f_{i(i+1)}(-\theta_i) = -f_{i(i+1)}(\theta_i)$ as indicated in Eq. (4), it can be found that maps m_9 to m_{16} in Table 2 are the negative angle forms of maps m_1 to m_8, and for each of the maps there are 16 types of combinations of the twist angles providing 16 variations of spherical 4R linkage. Figure 2 indicates the generation of the variations of the spherical 4R linkage, and the maps m_1 to m_8 are derived and the detailed combinations of twist angles $\alpha_{(i+j)(i+j+1)}$, $-\alpha_{(i+j)(i+j+1)}$, $\pi - \alpha_{(i+j)(i+j+1)}$, and $-\pi + \alpha_{(i+j)(i+j+1)}$ that lead to these maps are listed in Table A1 in **Appendix A**. Combinations of twist angles for maps m_9 to m_{16} are the same as those for maps m_1 to m_8, correspondingly. From Table 1, one can find that for each map m_i, there are 16 types of variations of spherical 4R linkage with various specified twist angles, and the 16 maps in Table 2 lead to 256 types (which may not all be different) of variations of special spherical 4R linkage of special twist angles; each denoted as v_{ij}: m_i-c_j, with i = 1 to 16 and j = 1 to 16 as shown in Fig. 2.

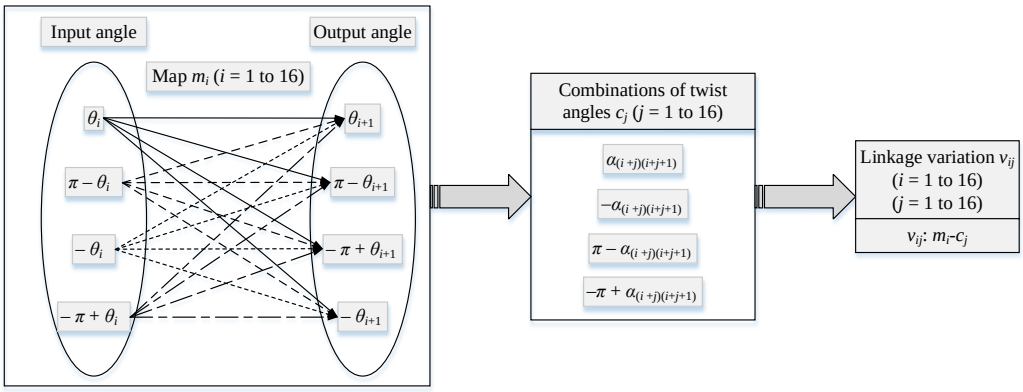

Figure 2 Generation of variations of spherical 4R linkage

By forming combinations of four of the variations of spherical 4R linkage from these 256 special spherical 4R linkages, various mobile assemblies of 1-DOF can be obtained which can then result in the corresponding origami patterns for the constructed of novel tessellations.

3. 1-DOF Mobile Assemblies of Four-spherical-4R-integrated Linkages

3.1 The Basic Assemblies of Spherical 4R Linkages

A mobile assembly of linkages is a network or tessellation of unit linkages with very few degrees of freedom (DOF) [29]. In order to construct 1-DOF mobile assemblies with four spherical 4R linkages,

the assembly of two spherical 4R linkages is considered first, and the connection between two spherical 4R linkages is constructed through the alignment and merging of a pair of common revolute joints from the two linkages as shown in Fig. 3. By defining the link between the i and i+1 joints in the spherical 4R linkage as link i(i+1), referring to Fig. 3, it can be seen that when joint a_1 in linkage A and joint b_1 in linkage B are aligned and merged, link 12 of linkage A and link 41 of linkage B are rigidly connected and become one link, and so are the link 14 of linkage A and link 12 of linkage B. This combination leads to the result that $\theta_1^a = \theta_1^b$; according to [15, 30] this is a two-spherical-4R-integrated linkage of 1 degree of freedom.

Similarly, by adding two more spherical 4R linkages, and aligning and merging the joints with the same subscript as shown in Fig. 4, an assembly of four spherical 4R linkages is obtained, which forms a four-spherical-4R-integrated linkage expected to be 1-DOF. In the linkage, joints a_1 and a_2 in linkage A is merged with joint d_1 of linkage D and joint b_2 of linkage B, respectively; and joints c_3 and c_4 in linkage C blend with joint b_3 of linkage B and joint d_4 of linkage D, respectively.

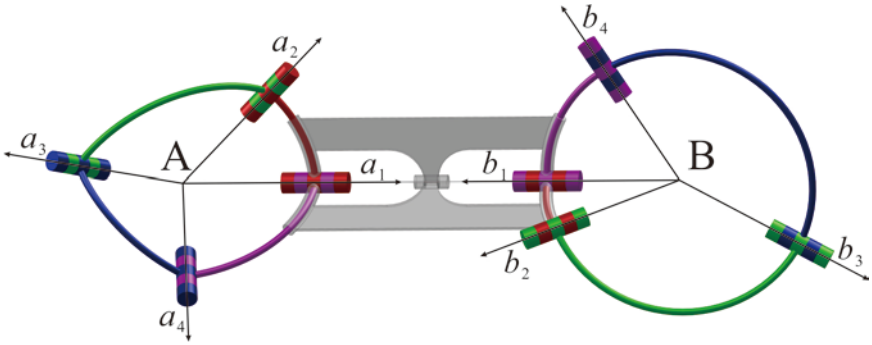

Figure 3 The assembly of two spherical 4R linkages.

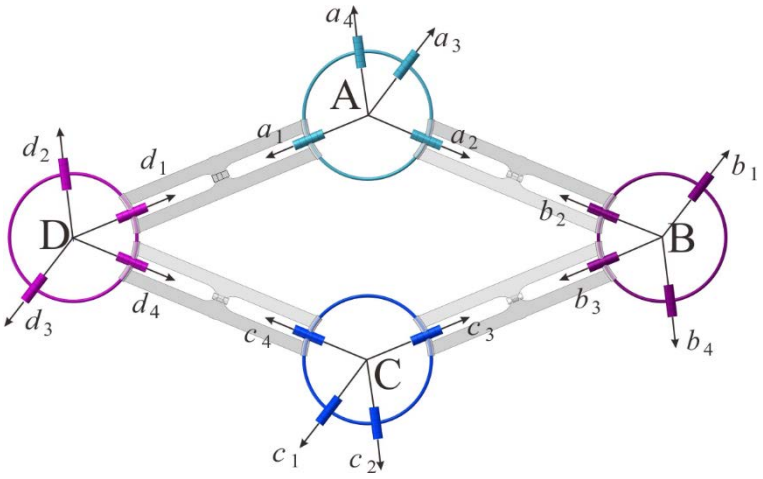

Figure 4 The assembly of four spherical 4R linkages.

For the sake of simplicity, we assumed that the four assembled spherical 4R linkages are identical such that there exist

$$
\begin{aligned}
&\alpha_{12}^{a} = \alpha_{12}^{b} = \alpha_{12}^{c} = \alpha_{12}^{d} = \alpha_{12},\\
&\alpha_{23}^{a} = \alpha_{23}^{b} = \alpha_{23}^{c} = \alpha_{23}^{d} = \alpha_{23},\\
&\alpha_{34}^{a} = \alpha_{34}^{b} = \alpha_{34}^{c} = \alpha_{34}^{d} = \alpha_{34},\\
&\alpha_{41}^{a} = \alpha_{41}^{b} = \alpha_{41}^{c} = \alpha_{41}^{d} = \alpha_{41}.
\end{aligned}
\tag{5}
$$

Based on this assumption, considering the four twist angles α_{12}^{k}, α_{23}^{k}, α_{34}^{k}, and α_{41}^{k} there are four types of the assemblies of four-spherical-4R-integrated linkages as shown in Fig. 5.

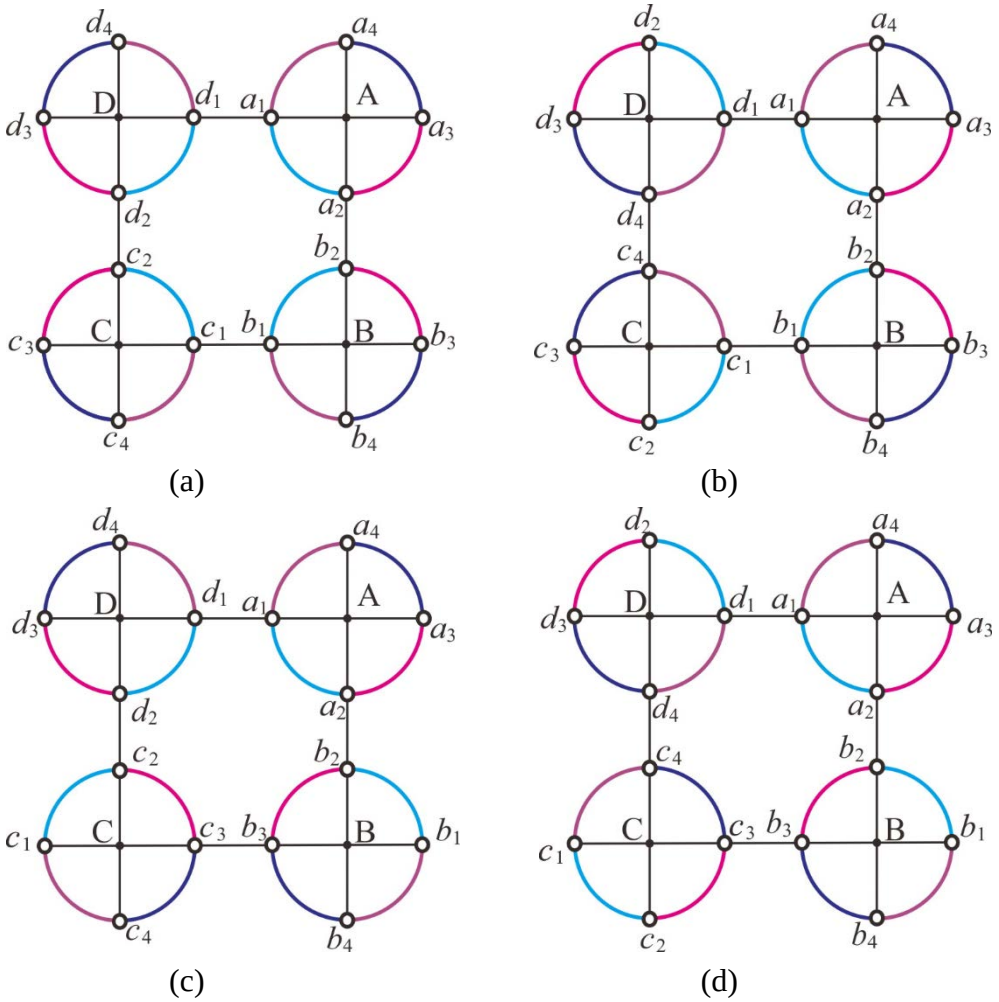

Figure 5 The schematic diagram of the assemblies of spherical 4R linkages: (a) double-plane symmetric case; (b) and (c) plane symmetric case; (d) rotational case (in which the straight lines represent the axes of the joints; the curved lines represent the links, and the nodes on the curved lines are the joints connecting the ends of the links.)

In Fig. 5(a) with the three-dimensional configuration supported in Fig. 6, the distribution of spherical 4R linkages C and D are the mirror of linkages A and B in the vertical direction, and in the meaning while linkages B and C are the mirror of linkages A and D in the horizontal direction, hence this is a *double-plane symmetric case*, which means it is planar-symmetric with respect to two orthogonal planes, i.e. plane hh' and vv' in Fig. 6. In order to keep this assembly to be one degree of freedom,

the kinematical compatibility conditions must be set up. Referring to Fig. 6, if θ_1^a is the input, using Eqs. (3) and (4) it has $-\theta_2^b = \theta_2^a = f_{12}^a(\theta_1^a)$, $-\theta_1^c = \theta_1^b = f_{21}^b(\theta_2^b)$, $-\theta_2^d = \theta_2^c = f_{12}^c(\theta_1^c)$ and $-\theta_1^a = \theta_1^d = f_{21}^d(\theta_2^d)$, in which the subscripts in f_{ij}^k indicate the input and output angles, e. g., f_{21}^b means that in the spherical 4R linkage B, the input angle is θ_2 and the output angle is θ_1. Thus, when the rotational motion transfers through the collinear joints, and back to θ_1^a in the end, the transmission loop can be expressed as

$$\begin{array}{l}(\theta_1^a)\rightarrow(\theta_2^a)=-(\theta_2^b)\rightarrow(\theta_1^b)=-(\theta_1^c)\rightarrow(\theta_2^c)=-(\theta_2^d)\rightarrow(\theta_1^d)\\ \uparrow\qquad\qquad\qquad\qquad\qquad\qquad\qquad\qquad\qquad\qquad\qquad\qquad\qquad\qquad\qquad\qquad\downarrow\\ \qquad\qquad\qquad\qquad\qquad\qquad(\theta_1^a)=-(\theta_1^d)\end{array} \tag{6}$$

which can be represent as $\theta_1^a = -f_{21}^d(-f_{12}^c(-f_{21}^b(-f_{12}^a(\theta_1^a))))$. Considering that the four linkages A, B, C and D are identical, Eq. (6) is simplified as $\theta_1^a = -f_{21}(-f_{12}(-f_{21}(-f_{12}(\theta_1^a))))$, according to Eq. (4), and as long as this condition is satisfied, this double-plane symmetric case is of 1-DOF four-spherical-4R-integrated linkage.

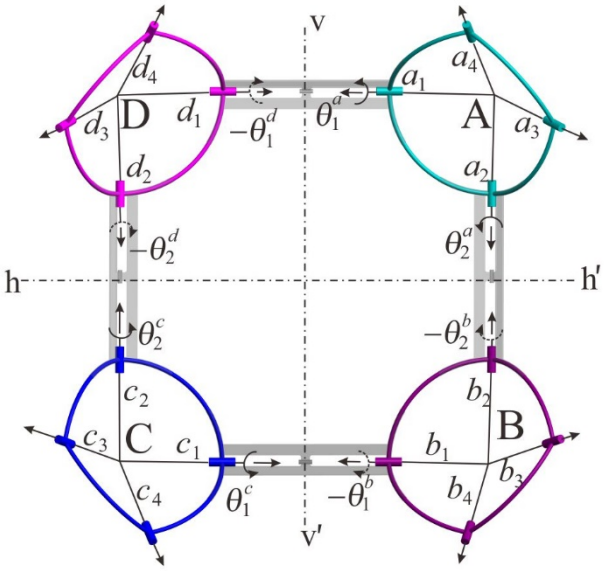

Figure 6 3D configuration of the assembly in double-plane symmetric case

Further, the distributions of spherical 4R linkages A and D, B and C are symmetric in the horizontal direction in Fig. 5(b); and the distributions of linkages A and B are symmetric with D and C in the vertical direction in Fig. 5c. Since these two cases have the same symmetric characteristics, the

assemblies in Fig. 5(b) and (c) are topologically the same, and are termed as *plane symmetric case*. Only Fig. 5(c) is taking into consideration in the following analysis and similar to the analysis for the double-plane symmetric case, the transmission loop for the plane symmetric case can be derived as

$$\begin{array}{c}(\theta_1^a)\rightarrow(\theta_2^a)=(\theta_2^b)\rightarrow(\theta_3^b)=-(\theta_3^c)\rightarrow(\theta_2^c)=(\theta_2^d)\rightarrow(\theta_1^d)\\ \uparrow\qquad\qquad\qquad

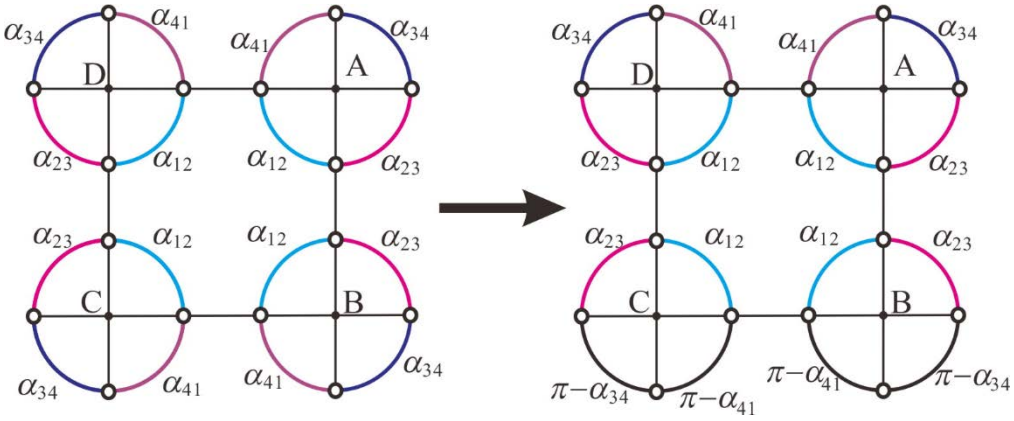

Figure 7 One variation of the double-plane symmetric case

The variants of the three basic assemblies are developed by maintaining the compatibility conditions for each case. In this development, twist angles in linkage D of each of the three basic assemblies are kept unchanged, and the variants are obtained by changing the twist angles of the other three linkages A, B, and C according to different maps and linkage variations derived in Section 2. Taking the double-plane symmetric case as an example as illustrated in Fig. 7, keep the twist angles in linkage D unchanged, and we change the twist angles in linkages B and C. Referring to the left figure in Fig. 7, in the original assembly, both linkages B and C satisfy map m_1 such that given θ_1 leads to θ_2 as $\theta_1 \rightarrow \theta_2$. After changing the twist angles in linkages B and C, assuming that the new linkages both obeying map m_{16} such that given $-\pi + \theta_1$ results in θ_2 as m_{16}: $-\pi + \theta_1$; a variant is obtained and illustrated on the right hand side of Fig. 7. And hence the transmission loop in equation for the new variant assembly then changes into

$$\begin{array}{l}(\theta_1^a)\rightarrow(\theta_2^a)=-(\theta_2^b)\rightarrow(-\pi+\theta_1^b)=-(-\pi+\theta_1^c)\rightarrow(\theta_2^c)=-(\theta_2^d)\rightarrow(\theta_1^d)\\ \uparrow \qquad\qquad\qquad\qquad (\theta_1^a)=-(\theta_1^d) \qquad\qquad\qquad\qquad \uparrow\end{array} \tag{9}$$

Comparing with Eq. (6), it is found that the transmission loop is changed in the intermediate process, but the compatibility condition $\theta_1^d = -\theta_1^a$ is still hold since linkage D is not changed, hence, this assembly is 1-DOF. One combination of the twist angles, which makes $\alpha_{i(i+1)} \in (0, \pi)$, for Eq. (9) according to Table A1 is

$$\begin{aligned}
&\alpha_{12}^a = \alpha_{12}^b = \alpha_{12}^c = \alpha_{12}^d = \alpha_{12}\\
&\alpha_{23}^a = \alpha_{23}^b = \alpha_{23}^c = \alpha_{23}^d = \alpha_{23}\\
&\alpha_{34}^a = \pi - \alpha_{34}^b = \pi - \alpha_{34}^c = \alpha_{34}^d = \alpha_{34}\\
&\alpha_{41}^a = \pi - \alpha_{41}^b = \pi - \alpha_{41}^c = \alpha_{41}^d = \alpha_{41}
\end{aligned} \tag{10}$$

And by changing the intermediate process of the transmission loop and keeping the compatibility condition $\theta_1^d = -\theta_1^a$, there are totally 15 different variations for the double-plane symmetric case,

which are enumerated and listed in Table 3, where v_{ti} represents the ith type of the variations of the double-plane symmetric case. The new types of linkages for A, B, C and D are given according to the different types of spherical 4R linkages provided in Appendix A, and n/c denotes that the linkage is not changed.

Table 3 Variants for the double-plane symmetric case

Variant types	Types of the four spherical 4R linkages			
	A	B	C	D
v_{t1}	m_2-c_i	m_2-c_i	n/c	n/c
v_{t2}	m_3-c_i	m_3-c_i	n/c	n/c
v_{t3}	m_4-c_i	m_4-c_i	n/c	n/c
v_{t4}	n/c	m_5-c_i	m_5-c_i	n/c
v_{t5}	n/c	m_{12}-c_i	m_{12}-c_i	n/c
v_{t6}	n/c	m_{16}-c_i	m_{16}-c_i	n/c
v_{t7}	m_2-c_i	m_6-c_i	m_5-c_i	n/c
v_{t8}	m_2-c_i	m_{15}-c_i	m_{16}-c_i	n/c
v_{t9}	m_2-c_i	m_{11}-c_i	m_{12}-c_i	n/c
v_{t10}	m_3-c_i	m_7-c_i	m_5-c_i	n/c
v_{t11}	m_3-c_i	m_{10}-c_i	m_{12}-c_i	n/c
v_{t12}	m_3-c_i	m_{14}-c_i	m_{16}-c_i	n/c
v_{t13}	m_4-c_i	m_8-c_i	m_5-c_i	n/c
v_{t14}	m_4-c_i	m_9-c_i	m_{12}-c_i	n/c
v_{t15}	m_4-c_i	m_{13}-c_i	m_{16}-c_i	n/c

Similarly, for the plane symmetric case, referring to Fig. 5(c) and let linkages A and B be replaced with linkages of types m_4-c_i and m_{12}-c_i respectively, an example of its variant can be obtained, and the corresponding new transmission loop equation can be derived as,

$$\begin{array}{c}(\theta_1^a)\rightarrow(-\theta_2^a)=(-\theta_2^b)\rightarrow(\theta_3^b)=-(\theta_3^c)\rightarrow(\theta_2^c)=(\theta_2^d)\rightarrow(\theta_1^d)\\ \uparrow\qquad\qquad\qquad\qquad (\theta_1^a)=-(\theta_1^d)\qquad\qquad\qquad\qquad\downarrow\end{array} \tag{11}$$

in which the compatibility condition $\theta_1^d = -\theta_1^a$ does not change. And one solution of the twist angles for spherical 4R linkages to constitute a network is

$$\begin{aligned}
\pi - \alpha_{12}^a &= \pi - \alpha_{12}^b = \alpha_{12}^c = \alpha_{12}^d = \alpha_{12} \\
\pi - \alpha_{23}^a &= \pi - \alpha_{23}^b = \alpha_{23}^c = \alpha_{23}^d = \alpha_{23} \\
\pi - \alpha_{34}^a &= \pi - \alpha_{34}^b = \alpha_{34}^c = \alpha_{34}^d = \alpha_{34} \\
\pi - \alpha_{41}^a &= \pi - \alpha_{41}^b = \alpha_{41}^c = \alpha_{41}^d = \alpha_{41}
\end{aligned} \tag{12}$$

This variant assembly of plane symmetric case is shown in Fig. 8. Similarly, using 16 kinds of variant geometric relationships can give more solutions for the twist angles. All variant relationships are listed in Table 4.

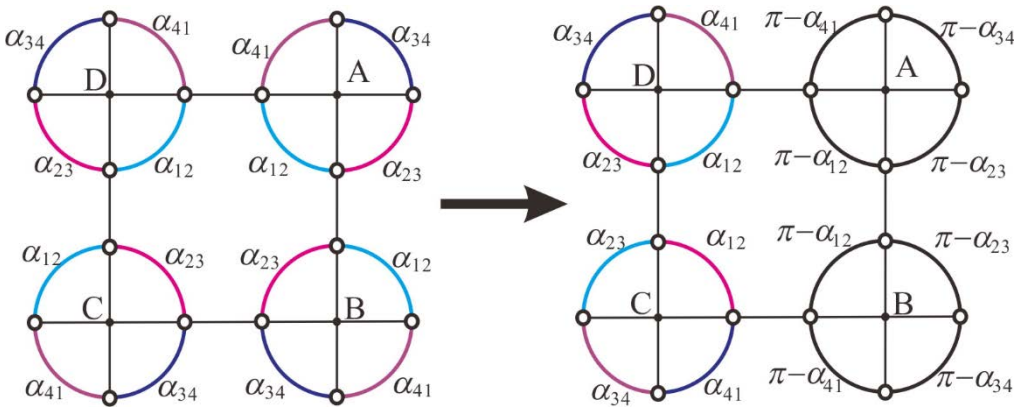

Figure 8 One variation of the plane symmetric case

Table 4 Variants for plane symmetric case.

Variant types	Types of the four spherical 4R linkages			
	A	B	C	D
v_{s1}	n/c	m_2-c_i	m_2-c_i	n/c
v_{s2}	n/c	m_3-c_i	m_3-c_i	n/c
v_{s3}	n/c	m_4-c_i	m_4-c_i	n/c
v_{s4}	m_2-c_i	m_5-c_i	n/c	n/c
v_{s5}	m_3-c_i	m_{16}-c_i	n/c	n/c
v_{s6}	m_4-c_i	m_{12}-c_i	n/c	n/c

v_{s7}	m_2-c_i	m_6-c_i	m_2-c_i	*n/c*
v_{s8}	m_2-c_i	m_7-c_i	m_3-c_i	*n/c*
v_{s9}	m_2-c_i	m_8-c_i	m_4-c_i	*n/c*
v_{s10}	m_3-c_i	m_{15}-c_i	m_2-c_i	*n/c*
v_{s11}	m_3-c_i	m_{14}-c_i	m_3-c_i	*n/c*
v_{s12}	m_3-c_i	m_{13}-c_i	m_4-c_i	*n/c*
v_{s13}	m_4-c_i	m_{11}-c_i	m_2-c_i	*n/c*
v_{s14}	m_4-c_i	m_{10}-c_i	m_3-c_i	*n/c*
v_{s15}	m_4-c_i	m_9-c_i	m_4-c_i	*n/c*

For rotational case, referring to Fig. 5(d), an example of the variant relationships, in which the compatibility condition $\theta_1^d = \theta_1^a$ remains, is by replacing linkage A with m_3-c_i, and linkage B with m_{16}-c_i; and the variant relationship is $\theta_1 \rightarrow -\pi + \theta_2$, and $-\pi + \theta_2 \rightarrow \theta_3$ and thus the transmission loop can be altered as

$$\begin{array}{l}(\theta_1^a)\rightarrow(-\pi+\theta_2^a)=(-\pi+\theta_2^b)\rightarrow(\theta_3^b)=(\theta_3^c)\rightarrow(\theta_4^c)=(\theta_4^d)\rightarrow(\theta_1^d)\\ \qquad\qquad\qquad\

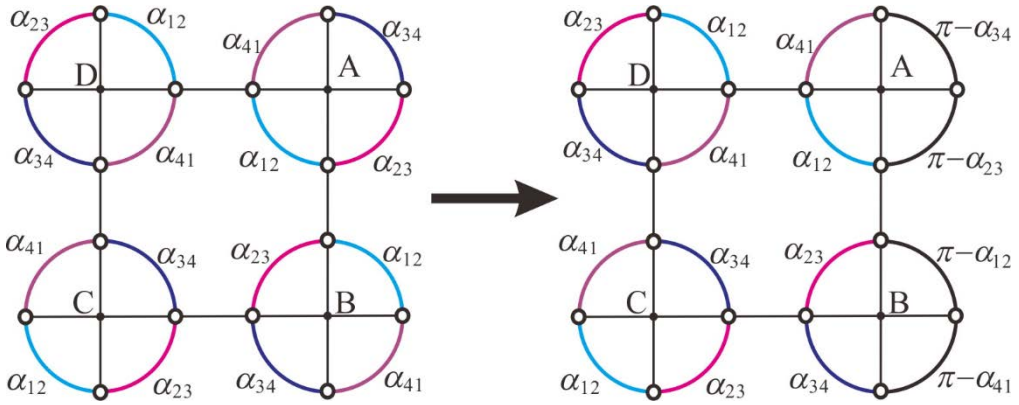

Fig. 9 One variation of the rotational case

Therefore, this section presents three basic assemblies of spherical 4R linkages and their variants and all these assemblies have their corresponding rigid origami patterns [24]. However, from the viewpoint of application, for each variation, those with twist angles satisfying $\alpha_{i(i+1)} \in (0, \pi)$ are considered in the following analysis, which are listed in Tables A2 (1)-(3) in Appendix A.

Table 5 Variants for rotational case

Variant types	Types of the four spherical 4R linkages			
	A	B	C	D
v_{r1}	m_2-c_i	m_5-c_i	*n/c*	*n/c*
v_{r2}	m_3-c_i	m_{16}-c_i	*n/c*	*n/c*
v_{r3}	m_4-c_i	m_{12}-c_i	*n/c*	*n/c*
v_{r4}	m_2-c_i	m_6-c_i	m_5-c_i	*n/c*
v_{r5}	m_2-c_i	m_7-c_i	m_{16}-c_i	*n/c*
v_{r6}	m_2-c_i	m_8-c_i	m_{12}-c_i	*n/c*
v_{r7}	m_3-c_i	m_{13}-c_i	m_{12}-c_i	*n/c*
v_{r8}	m_3-c_i	m_{14}-c_i	m_{16}-c_i	*n/c*
v_{r9}	m_3-c_i	m_{15}-c_i	m_5-c_i	*n/c*
v_{r10}	m_4-c_i	m_9-c_i	m_{12}-c_i	*n/c*
v_{r11}	m_4-c_i	m_{10}-c_i	m_{16}-c_i	*n/c*
v_{r12}	m_4-c_i	m_{11}-c_i	m_5-c_i	*n/c*

4. A Novel Origami Pattern Obtained from the Variations

Based on the equivalence between linkage and rigid origami [9, 23, 24], for all the mobile assemblies of the four-spherical-4R-integrated linkages obtained in Section 3 there exist corresponding rigid origami patterns. However, for each equivalent rigid origami, besides the compatibility conditions for the mobile assemblies mentioned above, some extra conditions known as flat-foldability [25, 31] should be added.

4.1 Flat-foldability of Degree-4 Vertices

To form a rigid origami pattern, according to the flat-foldability condition proposed in [31] the panel ABCD in Fig. 5 should be a planar quadrilateral such that in double-plane symmetric case, there must exist

$$\alpha_{12}^{a} = \alpha_{12}^{b} = \alpha_{12}^{c} = \alpha_{12}^{d} = \frac{\pi}{2}; \tag{15a}$$

For the symmetric case, there twist angles must satisfy

$$\alpha_{12}^{a} = \alpha_{12}^{d} = \pi - \alpha_{23}^{c} = \pi - \alpha_{23}^{b}, \tag{15b}$$

and for the rotational case, it complies with

$$\alpha_{12}^{a} + \alpha_{23}^{b} + \alpha_{34}^{c} + \alpha_{41}^{d} = 2\pi\,. \tag{15c}$$

Further, if a pattern is flat-deployable, i.e., the pattern can be folded from a flat paper, except for the rotational case, the addition conditions is

$$\alpha_{12}^{k} + \alpha_{23}^{k} + \alpha_{34}^{k} + \alpha_{41}^{k} = 2\pi \tag{16}$$

Where $\alpha_{i(i+1)}^{k} \in (0, 2\pi)$ with k stands for *a*, *b*, *c* and *d*.

In this way, we can derive the four-spherical-4R-integrated linkage from a desired pattern. Take the pattern of the bottom of the shopping bag in [13] as an example, and the folding process of the pattern is illustrated in Fig 10(a): The pattern belongs to the double-planesymmetric case, and its twist angles are shown in Fig. 10(b); according to Eqs. (5) and (15a), we can derive that $\alpha_{12}^{k} = \frac{\pi}{2}$. Since the pattern can be folded to a plane and deployed to a cuboid, we can also derive that $\alpha_{23}^{k} = \frac{\pi}{2}$ and $\alpha_{34}^{k} = \alpha_{41}^{k} = \frac{\pi}{4}$.

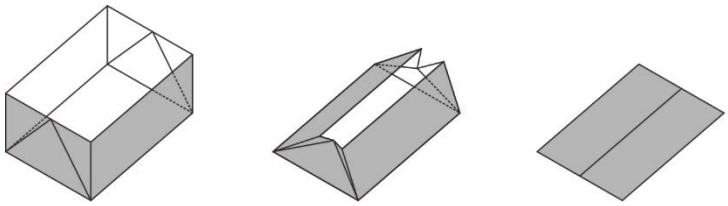

(a)

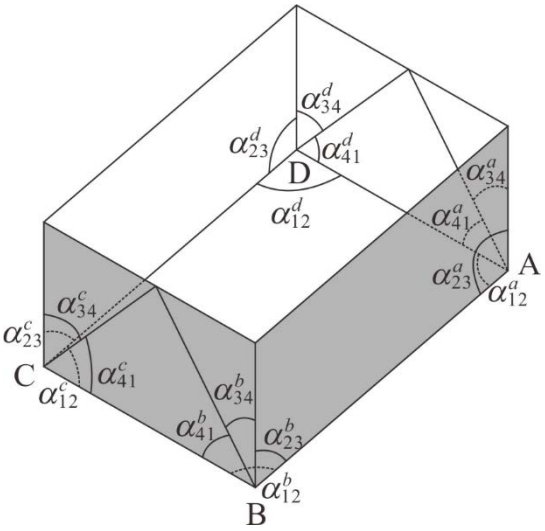

(b)

Figure 10 The shopping bag pattern, (a) the folding process and (b) the twist angles of the pattern

4.2 From Mobile Assemblies to Rigid Origami Patterns

Through the analogy between the linkage and the origami pattern, the origami patterns corresponding to all the three basic assemblies in Fig. 5 can be obtained. From the four-spherical-4R-integrated linkages, a general origami pattern with four-crease vertexes can be generated as illustrated in Fig. 10a. Here the creases surrounding vertex A, i.e., AD, AB, AE_2 and AE_1, correspond to joints a_1 to a_4 of the spherical 4R linkage A in Fig. 5, respectively. Similarly, the creases surrounding the other three vertexes correspond to the joints of the other three spherical 4R linkages in Fig. 5. Further, by setting the sector angles between the adjacent creases of the origami patterns according to the twist angles in the corresponding mobile assemblies, origami patterns stemming from the double-plane symmetric case, the symmetric case, and the rotational case can be obtained. Taking the rotational case as an example, by setting the sector angles $\alpha_{i(i+1)}^{k}$ according to the twist angles illustrated in Fig. 5(d), the corresponding origami pattern can be generated and sketched as shown in Fig. 11(a).

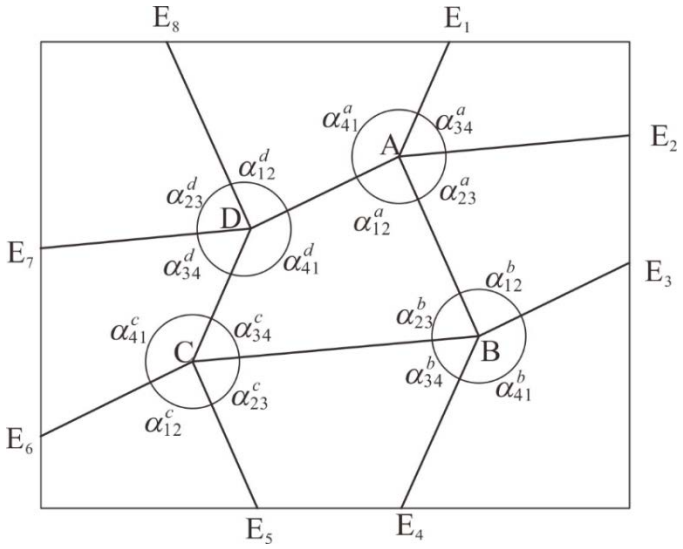

(a)

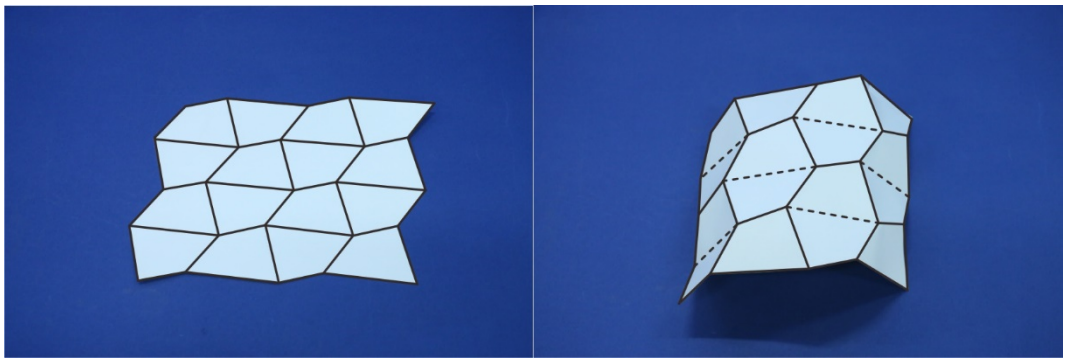

(b)

Figure 11 An origami pattern inspired by rotational case, (a) the origami pattern and (b) the physical model obtained from the rotational case.

When the corresponding assembly of the spherical 4R linkages meets the compatibility conditions, the origami pattern is rigid; and to become a rigid origami pattern, conditions for flat-foldability [28] must be satisfied, and combining Eqs. (8), (15c) and (16) one solution for the origami pattern in Fig. 11(a) can be derived as

$$\begin{aligned}
&\alpha_{12}^{a}=\alpha_{12}^{b}=\alpha_{12}^{c}=\alpha_{12}^{d}=\frac{\pi}{2}\\
&\alpha_{23}^{a}=\alpha_{23}^{b}=\alpha_{23}^{c}=\alpha_{23}^{d}=\frac{7\pi}{18}\\
&\alpha_{34}^{a}=\alpha_{34}^{b}=\alpha_{34}^{c}=\alpha_{34}^{d}=\frac{\pi}{3}\\
&\alpha_{41}^{a}=\alpha_{41}^{b}=\alpha_{41}^{c}=\alpha_{41}^{d}=\frac{7\pi}{9}
\end{aligned} \tag{17}$$

Using the solution in Eq. (17), a rigid origami pattern is generated and a physical model in a 4×4

tessellation form is made as shown in Fig. 11(b).

Further, if we alter the sector angles in the vertexes in Fig. 10(a) by replacing sector angles for vertex A with variation type v_{42}: m_4-c_2, and changing sector angles for vertexes B and C into variation type v_{91}: m_9-c_1 and type v_{122}: m_{12}-c_2, respectively, a new origami pattern can be evolved as show in Fig. 12(a). From derivation for the corresponding assembly, transmission loop equation for this new pattern is

$$\begin{array}{c} (\theta_1^a)\rightarrow(-\theta_2^a)=(-\theta_2^b)\rightarrow(-\theta_3^b)=(-\theta_3^c)\rightarrow(\theta_4^c)=(\theta_4^d)\rightarrow(\theta_1^d) \\ \uparrow \qquad\qquad\qquad\qquad (\theta_1^a)=(\theta_1^d) \qquad\qquad\qquad\qquad \downarrow \end{array} \tag{18}$$

Considering the cases listed in Table A2 in Appendix A, a solution for this pattern can be obtained as

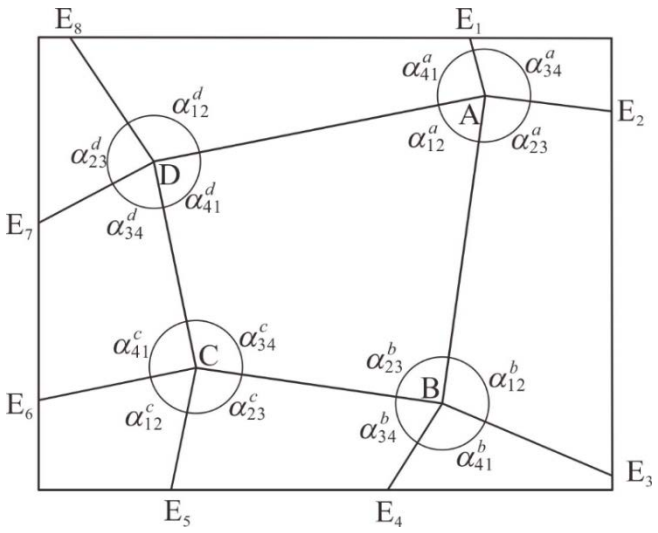

(a)

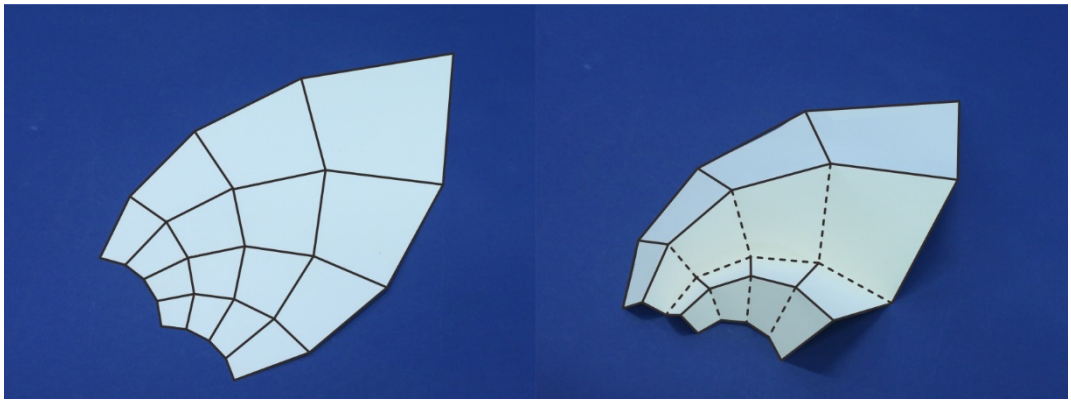

(b)

Figure. 12 An origami pattern generated from the variant of the rotational case, (a) a new the helical pattern, and (b) the physical model obtained from the rotational case's variation

$$\begin{aligned}
&\pi-\alpha_{12}^{a}=\alpha_{12}^{b}=\pi-\alpha_{12}^{c}=\alpha_{12}^{d}=\alpha_{12}\\
&\pi-\alpha_{23}^{a}=\alpha_{23}^{b}=\pi-\alpha_{23}^{c}=\alpha_{23}^{d}=\alpha_{23}\\
&\pi-\alpha_{34}^{a}=\alpha_{34}^{b}=\pi-\alpha_{34}^{c}=\alpha_{34}^{d}=\alpha_{34}\\
&\pi-\alpha_{41}^{a}=\alpha_{41}^{b}=\pi-\alpha_{41}^{c}=\alpha_{41}^{d}=\alpha_{41}
\end{aligned} \tag{19}$$

Substituting Eqs. (15c) and (17) into Eq. (19) leads to

$$\begin{aligned}
&\alpha_{12}+\alpha_{23}+\alpha_{34}+\alpha_{41}=2\pi,\\
&\alpha_{12}+\alpha_{34}=\pi,\alpha_{23}+\alpha_{41}=\pi.
\end{aligned} \tag{20}$$

Equations (19) and (20) provide the relationships between the twist angles in the new pattern, and considering the flat-foldability condition, a solution for this new rigid origami pattern is

$$\begin{aligned}
&\alpha_{12}^{a}=\alpha_{12}^{c}=\frac{\pi}{2},\quad \alpha_{12}^{b}=\alpha_{12}^{d}=\frac{\pi}{2},\\
&\alpha_{23}^{a}=\alpha_{23}^{c}=\frac{11}{18},\quad \alpha_{23}^{b}=\alpha_{23}^{d}=\frac{7\pi}{18},\\
&\alpha_{34}^{a}=\alpha_{34}^{c}=\frac{\pi}{2},\quad \alpha_{34}^{b}=\alpha_{34}^{d}=\frac{\pi}{2},\\
&\alpha_{41}^{a}=\alpha_{41}^{c}=\frac{7}{18},\quad \alpha_{41}^{b}=\alpha_{41}^{d}=\frac{11\pi}{18}.
\end{aligned} \tag{21}$$

Using this solution, a physical model of the new pattern is produced and illustrated in Fig. 12(b). This is a new rigid origami pattern and is termed a *helical pattern* in this paper.

4.3 Geometry of the New Helical Pattern

Geometry of the helical pattern is illustrated in Fig. 13. Figure 13(a) illustrates the lengths of the sides, in which a_i and b_i represents the row and column in which the sides in the latitude and longitude directions locate; a_{ij} and b_{ij} represents the length of the sides in the latitude and longitude directions, e. g. a_{33} is the length of the third side in row a_3 and b_{33} is the length of the third side in row b_3. The length of the sides in a single panel is shown in Fig. 13(b), in which there exist

$$a_{(i+1)j}=\sin(\alpha_{23}-\arcsin(\frac{b_{ij}}{m}))\cdot m \tag{22a}$$

$$b_{(i+1)j}=\sin(\alpha_{41}-\arcsin(\frac{a_{ij}}{m}))\cdot m \tag{22b}$$

$$\text{and} \quad m = \sqrt{a_{ij}^2 + b_{ij}^2 - 2a_{ij}b_{ij}\cos\alpha_{12}} \tag{22c}$$

In Fig. 13(c), the dihedral angles between neighboring panels in a single unit, ϕ_1 to ϕ_4 is illustrated and it has

$$\phi_1 = \phi_3, \phi_2 = \phi_4, \quad \text{and} \tag{23a}$$

$$\frac{\tan\frac{\phi_2}{2}}{\tan\frac{\phi_1}{2}} = -\frac{\sin\alpha_{12} - \sin\alpha_{23}}{\sin\alpha_{12} + \sin\alpha_{23}}. \tag{23b}$$

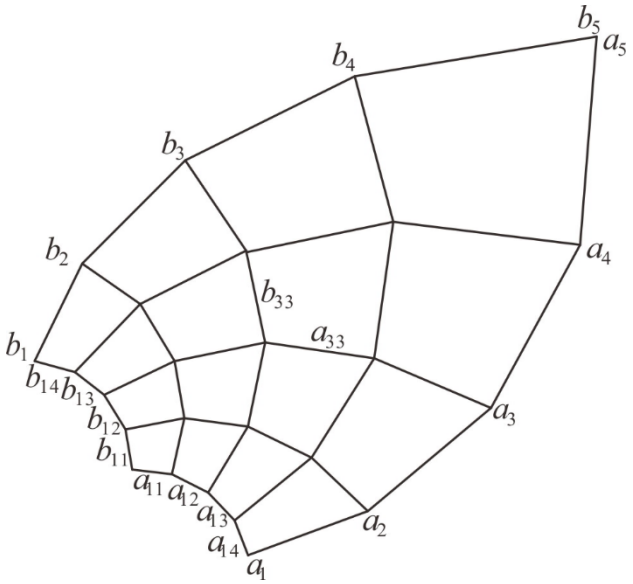

(a)

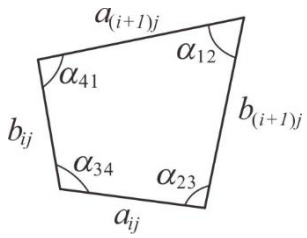

(b)

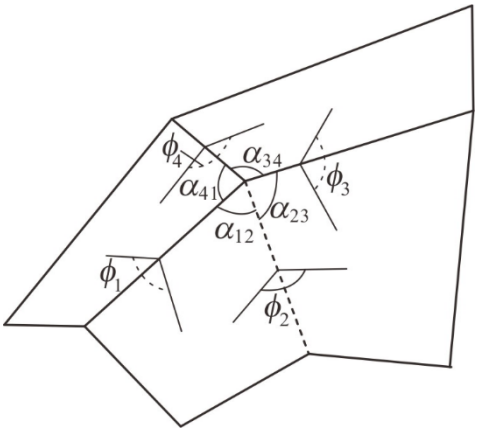

(c)

Figure 13 The geometry of the helical pattern: (a) the lengths of the sides; (b) a single panel and (c) the dihedral angles in a single unit.

Similar to the process of designing the novel helical origami pattern above, using the same analogy between linkage/mobile assembly and origami, it is supposed that all the mobile assemblies obtained in Section 3 can be used to identify and design their corresponding origami patterns. However, to from flat-foldable origami, the flat-foldability conditions presented in Section 4.1 must be satisfied. Hence, by using the variants of the mobile assemblies obtained in Section 3 as listed in Tables A2 (1) to (3) in Appendix A, and considering the flat-foldability conditions in Eqs. (15) and (16), all flat-deployable origami patterns (in which the twists $\alpha_{ij} \in (0, \pi)$) that can be found are derived and listed in Tables A3 (1) to (3). 18 flat-foldable origami patterns are obtained from the mobile assemblies of the double-plane symmetric, and plane symmetric cases, and 4 are obtained from the rotational case. According to the categories proposed in Ref. [22], for the 9 patterns from the double-plane symmetric case, 5 are planar symmetric type, 3 are supplementary type and 1 is translational type; for the 9 from the symmetric case, 3 are planar symmetric type, 3 are supplementary type and 3 are translational type; and for the 4 from rotational case, 1 is supplementary type and 3 belongs to the translational type. The helical pattern discovered in Section 4.2 is a novel pattern type.

5. Conclusions

This paper has proposed an innovative approach for synthesizing novel rigid origami patterns. Based on the kinematics of a single loop spherical 4R linkage, by assigning four pairs of specified input-output maps and by modifying the twist angles each with 4 specified values, 16 different maps between the specified input and output were obtained; and in each of the maps 16 combinations of the twist angles leading to 16 linkage types; these result in 256 special spherical 4R linkages. Then by integrating four spherical 4R linkages into one mobile assembly loop, three basic mobile assemblies containing four identical spherical 4R linkages were constructed. Kinematics of spherical 4R linkages was used to prove the mobility and the compatibility conditions among the assemblies and transmission loop equations of the basic assemblies were established altered. Further, by altering the vertex linkages of the three basic assemblies with the 256 special spherical 4R linkages, variations of them and suitable parameters of spherical 4R linkages were identified and the evolved transmission

loop equations were formed. Consequently, using the equivalence between the linkage and rigid origami, by combining the kinematic compatibility conditions of the mobile assemblies and geometrical conditions of origami patterns, from the assemblies obtained in this paper new rigid origami patterns were achieved with discovery of the novel helical pattern; which leads to the construction of novel tessellations. The theory proposed in the paper can lead to a large number of mobile assemblies of spherical 4R linkages, and using these assemblies associated with the equivalent rigid origami patterns, it is expected that novel origami structures and tessellations are to be found.

References

[1] Onal, C.D., Wood, R.J. and Rus, D. 2011, "Towards Printable Robotics: Origami-inspired Planar Fabrication of Three-dimensional Mechanisms," In Robotics and Automation (ICRA), 2011 IEEE International Conference on, pp. 4608-4613. May 9-13, 2011, Shanghai, China. (doi: 10.1109/ICRA.2011.5980139)

[2] Onal, C. D., Wood, R. J. and Rus, D. 2013, "An Origami-Inspired Approach to Worm Robots," IEEE/ASME TRANSACTIONS ON MECHATRONICS 18 430-438. (doi: 10.1109/TMECH.2012.2210239)

[3] Zirbel, S. A., Lang, R. J. and Thomson, M., W. 2013, "Accommodating Thickness in Origami-Based Deployable Arrays," In ASME 2013 international Design Engineering Technical Conferences and Computers and Information in Engineering Conference. 4-7 August 2013, Portland, Oregon, USA.

[4] Miyashita, S., Onal, C. D. and Rus, D. 2013, "Self-pop-up Cylindrical Structure by Global Heating," In 2013 IEEE/RSJ International Conference on Intelligent Robots and Systems (IROS), pp. 4065-4071. 3-7 Nov 2013, Tokyo, Japan.(doi: 10.1109/IROS.2013.6696938)

[5] Miura, K., 1989, "A Note on the Intrinsic Geometry of Origami," I Research of Pattern Formation, KTK Scientific Publishers, Tokyo, Japan: 91-102.

[6] Watanabe, N. and Kawaguchi, K. I., 2009, "The Method for Judging Rigid Foldability. In Origami 4, pp. 165-174, A K Peters/CRC Press.

[7] Hull, T. C., and Tachi, T. 2017, "Double-line Rigid Origami," arXiv preprint arXiv:1709.03210.

[8] He, Z., and Guest, S. D., 2018, "On Rigid Origami II: Quadrilateral Creased Papers," arXiv preprint arXiv:1804.06483.

[9] Dai, J. S., and Jones, J. R., 1999, "Mobility in Metamorphic Mechanisms of Foldable/Erectable Kinds," Journal of Mechanical Design, 121(3), 375-382.

[10] Stachel, H., 2010, "A Kinematic Approach to Kokotsakis Meshes." Computer Aided Geometric Design **27**, 428-437. (doi:10.1016/j.cagd.2010.05.002).

[11] Medellín-Castillo, H. I., and Cervantes-Sánchez, J. J., 2005, “An Improved Mobility Analysis for Spherical 4R Linkages,” Mechanism And Machine Theory, 40(8), pp. 931–947.

[12] Chiang, C. H., 1984, “On the Classification of Spherical Four-Bar Linkages,” Mechanism And Machine Theory, 19(3), pp. 283–287.

[13] Wu, W. N., and You, Z., 2011, “A Solution for Folding Rigid Tall Shopping Bags,” In Proceedings of the Royal Society of London A: Mathematical, Physical and Engineering Sciences, 467(2133) pp. 2561-2574. The Royal Society.

[14] Zhang, K. and Dai, J.S., 2013, “Classification of Origami-Enabled Foldable Linkages and Emerging Applications,” In ASME 2013 international Design Engineering Technical Conferences and Computers and Information in Engineering Conference. 4-7 August 2013, Portland, Oregon, USA.

[15] Wei, G. W., and Dai, J. S., 2014, “Origami-Inspired Integrated Planar-Spherical Overconstrained Mechanisms,” ASME Journal of Mechanical Design, 136(5), p. 051003.

[16] Chen, Y., and You, Z., 2005, “Mobile Assemblies Based on the Bennett Linkage,” In Proceedings of the royal society of London A: Mathematical, Physical and Engineering Sciences, 461(2056), pp. 1229-1245). The Royal Society.

[17] Chen, Y., and You, Z., 2008, “On Mobile Assemblies of Bennett Linkages,” In Proceedings of the Royal Society of London A: Mathematical, Physical and Engineering Sciences 464(2093), pp. 1275-1293, The Royal Society.

[18] Liu, S. Y., and Chen, Y., 2009, “Myard Linkage and Its Mobile Assemblies,” Mechanism And Machine Theory, 44(10), pp. 1950–1963.

[19] Wang, K. F., and Chen, Y., 2010, “Rigid Origami to Fold A Flat Paper into A Patterned Cylinder,” Origami 5: Fifth International Meeting of Origami Science, Mathematics, and Education, Singapore

[20] Zhang, X, and Chen, Y., 2018, “Mobile assemblies of Bennett linkages from four-crease origami patterns,” Proceedings of the Royal Society A: Mathematical, Physical and Engineering Sciences, 474(2210): 20170621.

[21] Liu, S., 2014, “Deployable Structure Associated with Rigid Origami and Its Mechanics”, PhD thesis, School of Mechanical and Aerospace Engineering, Nanyang Technological University, Singapore, 2014.

[22] Liu, S., Lv, W., Chen, Y., and Lu, G., 2016, “Deployable Prismatic Structures with Rigid Origami Patterns,” Journal of Mechanisms and Robotics, 8(3), 031002.

[23] Chen, Y., Lv, W., Li, J., and You, Z. 2017, “An Extended Family of Rigidly Foldable Origami Tubes,” Journal of Mechanisms and Robotics, 9(2), 021002.

[24] Cundy, H. M., and Rollett, A. P., 1952, “Mathematical Models,” Oxford University Press, New York.

[25] Wei, G. and Dai, J. S., 2009, “Geometry and Kinematic Analysis of an Origami-evolved Mechanism Based on Artmimetics, ”Advances in Reconfigurable Mechanisms and Robots, edited by Jian S Dai, Matteo Zoppi, and Xianwen Kong, KC Edizioni, pp. 450-455.

[26] Evans, T.A., Lang, R.J., Magleby, S.P. and Howell, L.L., 2015, “Rigidly foldable origami gadgets and tessellations”. Royal Society Open Scinece, 2, 150067.

[27] Denavit, J. and Hartenberg, R. S. 1955, “A Kinematic Notation for Lower-pair MechanismsBased on Matrices,” Journal of Applied Mechanics, Transactions of the ASME. 22, pp. 215–221.

[28] Feng H, Peng R, Ma J, et al., 2018 “Rigid foldability of generalized triangle twist origami pattern and its derived 6r linkages”, Journal of Mechanisms and Robotics, 10(5): 051003.

[29] You Z, Chen Y. 2012 Motion structures. London, UK: Spon Press.

[30] Qiu, C., Aminzadeh, V. and Dai, J.S., 2013, “Kinematic and stiffness analysis of an origami-type carton, ”Journal of Mechanical Design, Trans. ASME, 135 (11): 111004.

[31] Hull, T. C., 2003, “Counting mountain-valley assignments for flat folds”. Ars Combinatoria, 67, pp. 175-188.

Appendix A

Table A1 Maps, the associated combinations of twist angles and linkage variations

Map	Combinations of $\alpha_{(i+j)(i+j+1)}$, $-\alpha_{(i+j)(i+j+1)}$, $\pi-\alpha_{(i+j)(i+j+1)}$, $-\pi+\alpha_{(i+j)(i+j+1)}$	variants
m_1: $\theta_i \rightarrow \theta_{i+1}$	$\alpha_{i(i+1)}$, $\alpha_{(i+1)(i+2)}$, $\alpha_{(i+2)(i+3)}$, $\alpha_{(i+3)(i+4)}$	v_{11}: m_1-c_1
	$\alpha_{i(i+1)}$, $\alpha_{(i+1)(i+2)}$, $\pi-\alpha_{(i+2)(i+3)}$, $-\pi+\alpha_{(i+3)(i+4)}$	v_{12}: m_1-c_2
	$\alpha_{i(i+1)}$, $\alpha_{(i+1)(i+2)}$, $-\pi+\alpha_{(i+2)(i+3)}$, $-\pi+\alpha_{(i+3)(i+4)}$	v_{13}: m_1-c_3
	$\alpha_{i(i+1)}$, $\alpha_{(i+1)(i+2)}$, $-\alpha_{(i+2)(i+3)}$, $\alpha_{(i+3)(i+4)}$	v_{14}: m_1-c_4
	$\alpha_{i(i+1)}$, $-\pi+\alpha_{(i+1)(i+2)}$, $\alpha_{(i+2)(i+3)}$, $-\pi+\alpha_{(i+3)(i+4)}$	v_{15}: m_1-c_5
	$\alpha_{i(i+1)}$, $-\pi+\alpha_{(i+1)(i+2)}$, $\pi-\alpha_{(i+2)(i+3)}$, $\alpha_{(i+3)(i+4)}$	v_{16}: m_1-c_6
	$\alpha_{i(i+1)}$, $-\pi+\alpha_{(i+1)(i+2)}$, $-\pi+\alpha_{(i+2)(i+3)}$, $\alpha_{(i+3)(i+4)}$	v_{17}: m_1-c_7
	$\alpha_{i(i+1)}$, $-\pi+\alpha_{(i+1)(i+2)}$, $-\alpha_{(i+2)(i+3)}$, $-\pi+\alpha_{(i+3)(i+4)}$	v_{18}: m_1-c_8
	$-\alpha_{i(i+1)}$, $\pi-\alpha_{(i+1)(i+2)}$, $\alpha_{(i+2)(i+3)}$, $\pi-\alpha_{(i+3)(i+4)}$	v_{19}: m_1-c_9
	$-\alpha_{i(i+1)}$, $\pi-\alpha_{(i+1)(i+2)}$, $\pi-\alpha_{(i+2)(i+3)}$, $-\alpha_{(i+3)(i+4)}$	v_{110}: m_1-c_{10}
	$-\alpha_{i(i+1)}$, $\pi-\alpha_{(i+1)(i+2)}$, $-\pi+\alpha_{(i+2)(i+3)}$, $-\alpha_{(i+3)(i+4)}$	v_{111}: m_1-c_{11}
	$-\alpha_{i(i+1)}$, $\pi-\alpha_{(i+1)(i+2)}$, $-\alpha_{(i+2)(i+3)}$, $\pi-\alpha_{(i+3)(i+4)}$	v_{112}: m_1-c_{12}
	$-\alpha_{i(i+1)}$, $-\alpha_{(i+1)(i+2)}$, $\alpha_{(i+2)(i+3)}$, $-\alpha_{(i+3)(i+4)}$	v_{113}: m_1-c_{13}
	$-\alpha_{i(i+1)}$, $-\alpha_{(i+1)(i+2)}$, $\pi-\alpha_{(i+2)(i+3)}$, $\pi-\alpha_{(i+3)(i+4)}$	v_{114}: m_1-c_{14}
	$-\alpha_{i(i+1)}$, $-\alpha_{(i+1)(i+2)}$, $-\pi+\alpha_{(i+2)(i+3)}$, $\pi-\alpha_{(i+3)(i+4)}$	v_{115}: m_1-c_{15}
	$-\alpha_{i(i+1)}$, $-\alpha_{(i+1)(i+2)}$, $-\alpha_{(i+2)(i+3)}$, $-\alpha_{(i+3)(i+4)}$	v_{116}: m_1-c_{16}
m_2: $\theta_i \rightarrow \pi-\theta_{(i+1)}$	$\pi-\alpha_{i(i+1)}$, $\alpha_{(i+1)(i+2)}$, $\alpha_{(i+2)(i+3)}$, $\pi-\alpha_{(i+3)(i+4)}$	v_{21}: m_2-c_1
	$\pi-\alpha_{i(i+1)}$, $\alpha_{(i+1)(i+2)}$, $\pi-\alpha_{(i+2)(i+3)}$, $-\alpha_{(i+3)(i+4)}$	v_{22}: m_2-c_2
	$\pi-\alpha_{i(i+1)}$, $\alpha_{(i+1)(i+2)}$, $-\pi+\alpha_{(i+2)(i+3)}$, $-\alpha_{(i+3)(i+4)}$	v_{23}: m_2-c_3
	$\pi-\alpha_{i(i+1)}$, $\alpha_{(i+1)(i+2)}$, $-\alpha_{(i+2)(i+3)}$, $\pi-\alpha_{(i+3)(i+4)}$	v_{24}: m_2-c_4
	$\pi-\alpha_{i(i+1)}$, $\alpha_{(i+1)(i+2)}$, $-\pi+\alpha_{(i+2)(i+3)}$, $-\alpha_{(i+3)(i+4)}$	v_{25}: m_2-c_5
	$\pi-\alpha_{i(i+1)}$, $-\pi+\alpha_{(i+1)(i+2)}$, $\pi-\alpha_{(i+2)(i+3)}$, $\pi-\alpha_{(i+3)(i+4)}$	v_{26}: m_2-c_6
	$\pi-\alpha_{i(i+1)}$, $-\pi+\alpha_{(i+1)(i+2)}$, $-\pi+\alpha_{(i+2)(i+3)}$, $\pi-\alpha_{(i+3)(i+4)}$	v_{27}: m_2-c_7
	$\pi-\alpha_{i(i+1)}$, $-\pi+\alpha_{(i+1)(i+2)}$, $-\alpha_{(i+2)(i+3)}$, $-\alpha_{(i+3)(i+4)}$	v_{28}: m_2-c_8
	$-\pi+\alpha_{i(i+1)}$, $\pi-\alpha_{(i+1)(i+2)}$, $\alpha_{(i+2)(i+3)}$, $\alpha_{(i+3)(i+4)}$	v_{29}: m_2-c_9
	$-\pi+\alpha_{i(i+1)}$, $\pi-\alpha_{(i+1)(i+2)}$, $\pi-\alpha_{(i+2)(i+3)}$, $-\pi+\alpha_{(i+3)(i+4)}$	v_{210}: m_2-c_{10}
	$-\pi+\alpha_{i(i+1)}$, $\pi-\alpha_{(i+1)(i+2)}$, $-\pi+\alpha_{(i+2)(i+3)}$, $-\pi+\alpha_{(i+3)(i+4)}$	v_{211}: m_2-c_{11}
	$-\pi+\alpha_{i(i+1)}$, $\pi-\alpha_{(i+1)(i+2)}$, $-\alpha_{(i+2)(i+3)}$, $\alpha_{(i+3)(i+4)}$	v_{212}: m_2-c_{12}

	$-\pi+\alpha_{i(i+1)}, -\alpha_{(i+1)(i+2)}, \alpha_{(i+2)(i+3)}, -\pi+\alpha_{(i+3)(i+4)}$	v_{213}: m_2-c_{13}
	$-\pi+\alpha_{i(i+1)}, -\alpha_{(i+1)(i+2)}, \pi-\alpha_{(i+2)(i+3)}, \alpha_{(i+3)(i+4)}$	v_{214}: m_2-c_{14}
	$-\pi+\alpha_{i(i+1)}, -\alpha_{(i+1)(i+2)}, -\pi+\alpha_{(i+2)(i+3)}, \alpha_{(i+3)(i+4)}$	v_{215}: m_2-c_{15}
	$-\pi+\alpha_{i(i+1)}, -\alpha_{(i+1)(i+2)}, -\alpha_{(i+2)(i+3)}, -\pi+\alpha_{(i+3)(i+4)}$	v_{216}: m_2-c_{16}
m_3: $\theta_i \rightarrow -\pi+\theta_{(i+1)}$	$\alpha_{i(i+1)}, \pi-\alpha_{(i+1)(i+2)}, \alpha_{(i+2)(i+3)}, -\pi+\alpha_{(i+3)(i+4)}$	v_{31}: m_3-c_1
	$\alpha_{i(i+1)}, \pi-\alpha_{(i+1)(i+2)}, \pi-\alpha_{(i+2)(i+3)}, \alpha_{(i+3)(i+4)}$	v_{32}: m_3-c_2
	$\alpha_{i(i+1)}, \pi-\alpha_{(i+1)(i+2)}, -\pi+\alpha_{(i+2)(i+3)}, \alpha_{(i+3)(i+4)}$	v_{33}: m_3-c_3
	$\alpha_{i(i+1)}, \pi-\alpha_{(i+1)(i+2)}, -\alpha_{(i+2)(i+3)}, -\pi+\alpha_{(i+3)(i+4)}$	v_{34}: m_3-c_4
	$\alpha_{i(i+1)}, -\alpha_{(i+1)(i+2)}, \alpha_{(i+2)(i+3)}, \alpha_{(i+3)(i+4)}$	v_{35}: m_3-c_5
	$\alpha_{i(i+1)}, -\alpha_{(i+1)(i+2)}, \pi-\alpha_{(i+2)(i+3)}, -\pi+\alpha_{(i+3)(i+4)}$	v_{36}: m_3-c_6
	$\alpha_{i(i+1)}, -\alpha_{(i+1)(i+2)}, -\pi+\alpha_{(i+2)(i+3)}, -\pi+\alpha_{(i+3)(i+4)}$	v_{37}: m_3-c_7
	$\alpha_{i(i+1)}, -\alpha_{(i+1)(i+2)}, -\alpha_{(i+2)(i+3)}, \alpha_{(i+3)(i+4)}$	v_{38}: m_3-c_8
	$-\alpha_{i(i+1)}, \alpha_{(i+1)(i+2)}, \alpha_{(i+2)(i+3)}, -\alpha_{(i+3)(i+4)}$	v_{39}: m_3-c_9
	$-\alpha_{i(i+1)}, \alpha_{(i+1)(i+2)}, \pi-\alpha_{(i+2)(i+3)}, \pi-\alpha_{(i+3)(i+4)}$	v_{310}: m_3-c_{10}
	$-\alpha_{i(i+1)}, \alpha_{(i+1)(i+2)}, -\pi+\alpha_{(i+2)(i+3)}, \pi-\alpha_{(i+3)(i+4)}$	v_{311}: m_3-c_{11}
	$-\alpha_{i(i+1)}, \alpha_{(i+1)(i+2)}, -\alpha_{(i+2)(i+3)}, -\alpha_{(i+3)(i+4)}$	v_{312}: m_3-c_{12}
	$-\alpha_{i(i+1)}, -\pi+\alpha_{(i+1)(i+2)}, \alpha_{(i+2)(i+3)}, \pi-\alpha_{(i+3)(i+4)}$	v_{313}: m_3-c_{13}
	$-\alpha_{i(i+1)}, -\pi+\alpha_{(i+1)(i+2)}, \pi-\alpha_{(i+2)(i+3)}, -\alpha_{(i+3)(i+4)}$	v_{314}: m_3-c_{14}
	$-\alpha_{i(i+1)}, -\pi+\alpha_{(i+1)(i+2)}, -\pi+\alpha_{(i+2)(i+3)}, -\alpha_{(i+3)(i+4)}$	v_{315}: m_3-c_{15}
	$-\alpha_{i(i+1)}, -\pi+\alpha_{(i+1)(i+2)}, -\alpha_{(i+2)(i+3)}, \pi-\alpha_{(i+3)(i+4)}$	v_{316}: m_3-c_{16}
m_4: $\theta_i \rightarrow -\theta_{(i+1)}$	$\pi-\alpha_{i(i+1)}, \pi-\alpha_{(i+1)(i+2)}, \alpha_{(i+2)(i+3)}, -\alpha_{(i+3)(i+4)}$	v_{41}: m_4-c_1
	$\pi-\alpha_{i(i+1)}, \pi-\alpha_{(i+1)(i+2)}, \pi-\alpha_{(i+2)(i+3)}, \pi-\alpha_{(i+3)(i+4)}$	v_{42}: m_4-c_2
	$\pi-\alpha_{i(i+1)}, \pi-\alpha_{(i+1)(i+2)}, -\pi+\alpha_{(i+2)(i+3)}, \pi-\alpha_{(i+3)(i+4)}$	v_{43}: m_4-c_3
	$\pi-\alpha_{i(i+1)}, \pi-\alpha_{(i+1)(i+2)}, -\alpha_{(i+2)(i+3)}, -\alpha_{(i+3)(i+4)}$	v_{44}: m_4-c_4
	$\pi-\alpha_{i(i+1)}, -\alpha_{(i+1)(i+2)}, \alpha_{(i+2)(i+3)}, \pi-\alpha_{(i+3)(i+4)}$	v_{45}: m_4-c_5
	$\pi-\alpha_{i(i+1)}, -\alpha_{(i+1)(i+2)}, \pi-\alpha_{(i+2)(i+3)}, -\alpha_{(i+3)(i+4)}$	v_{46}: m_4-c_6
	$\pi-\alpha_{i(i+1)}, -\alpha_{(i+1)(i+2)}, -\pi+\alpha_{(i+2)(i+3)}, -\alpha_{(i+3)(i+4)}$	v_{47}: m_4-c_7
	$\pi-\alpha_{i(i+1)}, -\alpha_{(i+1)(i+2)}, -\alpha_{(i+2)(i+3)}, \pi-\alpha_{(i+3)(i+4)}$	v_{48}: m_4-c_8
	$-\pi+\alpha_{i(i+1)}, \alpha_{(i+1)(i+2)}, \alpha_{(i+2)(i+3)}, -\pi+\alpha_{(i+3)(i+4)}$	v_{49}: m_4-c_9
	$-\pi+\alpha_{i(i+1)}, \alpha_{(i+1)(i+2)}, \pi+\alpha_{(i+2)(i+3)}, \alpha_{(i+3)(i+4)}$	v_{410}: m_4-c_{10}
	$-\pi+\alpha_{i(i+1)}, \alpha_{(i+1)(i+2)}, -\pi+\alpha_{(i+2)(i+3)}, \alpha_{(i+3)(i+4)}$	v_{411}: m_4-c_{11}

	$-\pi + \alpha_{i(i+1)}, \alpha_{(i+1)(i+2)}, -\alpha_{(i+2)(i+3)}, -\pi + \alpha_{(i+3)(i+4)}$	v_{412}: m_4-c_{12}
	$-\pi + \alpha_{i(i+1)}, -\pi + \alpha_{(i+1)(i+2)}, \alpha_{(i+2)(i+3)}, \alpha_{(i+3)(i+4)}$	v_{413}: m_4-c_{13}
	$-\pi + \alpha_{i(i+1)}, -\pi + \alpha_{(i+1)(i+2)}, \pi - \alpha_{(i+2)(i+3)}, -\pi + \alpha_{(i+3)(i+4)}$	v_{414}: m_4-c_{14}
	$-\pi + \alpha_{i(i+1)}, -\pi + \alpha_{(i+1)(i+2)}, \pi + \alpha_{(i+2)(i+3)}, -\pi + \alpha_{(i+3)(i+4)}$	v_{415}: m_4-c_{15}
	$-\pi + \alpha_{i(i+1)}, -\pi + \alpha_{(i+1)(i+2)}, -\alpha_{(i+2)(i+3)}, \alpha_{(i+3)(i+4)}$	v_{416}: m_4-c_{16}
m_5: $\pi - \theta_i \rightarrow \theta_{(i+1)}$	$\pi - \alpha_{i(i+1)}, \pi - \alpha_{(i+1)(i+2)}, \alpha_{(i+2)(i+3)}, \alpha_{(i+3)(i+4)}$	v_{51}: m_5-c_1
	$\pi - \alpha_{i(i+1)}, \pi - \alpha_{(i+1)(i+2)}, \pi - \alpha_{(i+2)(i+3)}, -\pi + \alpha_{(i+3)(i+4)}$	v_{52}: m_5-c_2
	$\pi - \alpha_{i(i+1)}, \pi - \alpha_{(i+1)(i+2)}, -\pi + \alpha_{(i+2)(i+3)}, -\pi + \alpha_{(i+3)(i+4)}$	v_{53}: m_5-c_3
	$\pi - \alpha_{i(i+1)}, \pi - \alpha_{(i+1)(i+2)}, -\alpha_{(i+2)(i+3)}, \alpha_{(i+3)(i+4)}$	v_{54}: m_5-c_4
	$\pi - \alpha_{i(i+1)}, -\alpha_{(i+1)(i+2)}, \alpha_{(i+2)(i+3)}, -\pi + \alpha_{(i+3)(i+4)}$	v_{55}: m_5-c_5
	$\pi - \alpha_{i(i+1)}, -\alpha_{(i+1)(i+2)}, \pi - \alpha_{(i+2)(i+3)}, \alpha_{(i+3)(i+4)}$	v_{56}: m_5-c_6
	$\pi - \alpha_{i(i+1)}, -\alpha_{(i+1)(i+2)}, -\pi + \alpha_{(i+2)(i+3)}, \alpha_{(i+3)(i+4)}$	v_{57}: m_5-c_7
	$\pi - \alpha_{i(i+1)}, -\alpha_{(i+1)(i+2)}, -\alpha_{(i+2)(i+3)}, -\pi + \alpha_{(i+3)(i+4)}$	v_{58}: m_5-c_8
	$-\pi + \alpha_{i(i+1)}, \alpha_{(i+1)(i+2)}, \alpha_{(i+2)(i+3)}, \pi - \alpha_{(i+3)(i+4)}$	v_{59}: m_5-c_9
	$-\pi + \alpha_{i(i+1)}, \alpha_{(i+1)(i+2)}, \pi - \alpha_{(i+2)(i+3)}, -\alpha_{(i+3)(i+4)}$	v_{510}: m_5-c_{10}
	$-\pi + \alpha_{i(i+1)}, \alpha_{(i+1)(i+2)}, -\pi + \alpha_{(i+2)(i+3)}, -\alpha_{(i+3)(i+4)}$	v_{511}: m_5-c_{11}
	$-\pi + \alpha_{i(i+1)}, \alpha_{(i+1)(i+2)}, -\alpha_{(i+2)(i+3)}, \pi - \alpha_{(i+3)(i+4)}$	v_{512}: m_5-c_{12}
	$-\pi + \alpha_{i(i+1)}, -\pi + \alpha_{(i+1)(i+2)}, \alpha_{(i+2)(i+3)}, -\alpha_{(i+3)(i+4)}$	v_{513}: m_5-c_{13}
	$-\pi + \alpha_{i(i+1)}, -\pi + \alpha_{(i+1)(i+2)}, \pi - \alpha_{(i+2)(i+3)}, \pi - \alpha_{(i+3)(i+4)}$	v_{514}: m_5-c_{14}
	$-\pi + \alpha_{i(i+1)}, -\pi + \alpha_{(i+1)(i+2)}, -\pi + \alpha_{(i+2)(i+3)}, \pi - \alpha_{(i+3)(i+4)}$	v_{515}: m_5-c_{15}
	$-\pi + \alpha_{i(i+1)}, -\pi + \alpha_{(i+1)(i+2)}, -\alpha_{(i+2)(i+3)}, -\alpha_{(i+3)(i+4)}$	v_{516}: m_5-c_{16}
m_6: $\pi - \theta_i \rightarrow \pi - \theta_{(i+1)}$	$\alpha_{i(i+1)}, \pi - \alpha_{(i+1)(i+2)}, \alpha_{(i+2)(i+3)}, \pi - \alpha_{(i+3)(i+4)}$	v_{61}: m_6-c_1
	$\alpha_{i(i+1)}, \pi - \alpha_{(i+1)(i+2)}, \pi - \alpha_{(i+2)(i+3)}, -\alpha_{(i+3)(i+4)}$	v_{62}: m_6-c_2
	$\alpha_{i(i+1)}, \pi - \alpha_{(i+1)(i+2)}, -\pi + \alpha_{(i+2)(i+3)}, -\alpha_{(i+3)(i+4)}$	v_{63}: m_6-c_3
	$\alpha_{i(i+1)}, \pi - \alpha_{(i+1)(i+2)}, -\alpha_{(i+2)(i+3)}, \pi - \alpha_{(i+3)(i+4)}$	v_{64}: m_6-c_4
	$\alpha_{i(i+1)}, -\alpha_{(i+1)(i+2)}, \alpha_{(i+2)(i+3)}, -\alpha_{(i+3)(i+4)}$	v_{65}: m_6-c_5
	$\alpha_{i(i+1)}, -\alpha_{(i+1)(i+2)}, \pi - \alpha_{(i+2)(i+3)}, \pi - \alpha_{(i+3)(i+4)}$	v_{66}: m_6-c_6
	$\alpha_{i(i+1)}, -\alpha_{(i+1)(i+2)}, -\pi + \alpha_{(i+2)(i+3)}, \pi - \alpha_{(i+3)(i+4)}$	v_{67}: m_6-c_7
	$\alpha_{i(i+1)}, -\alpha_{(i+1)(i+2)}, -\alpha_{(i+2)(i+3)}, -\alpha_{(i+3)(i+4)}$	v_{68}: m_6-c_8
	$-\alpha_{i(i+1)}, \alpha_{(i+1)(i+2)}, \alpha_{(i+2)(i+3)}, \alpha_{(i+3)(i+4)}$	v_{69}: m_6-c_9
	$-\alpha_{i(i+1)}, \alpha_{(i+1)(i+2)}, \pi - \alpha_{(i+2)(i+3)}, -\pi + \alpha_{(i+3)(i+4)}$	v_{610}: m_6-c_{10}

	$-\alpha_{i(i+1)}, \alpha_{(i+1)(i+2)}, -\pi+\alpha_{(i+2)(i+3)}, -\pi+\alpha_{(i+3)(i+4)}$	v_{611}: m_6-c_{11}
	$-\alpha_{i(i+1)}, \alpha_{(i+1)(i+2)}, -\alpha_{(i+2)(i+3)}, \alpha_{(i+3)(i+4)}$	v_{612}: m_6-c_{12}
	$-\alpha_{i(i+1)}, -\pi+\alpha_{(i+1)(i+2)}, \alpha_{(i+2)(i+3)}, -\pi+\alpha_{(i+3)(i+4)}$	v_{613}: m_6-c_{13}
	$-\alpha_{i(i+1)}, -\pi+\alpha_{(i+1)(i+2)}, \pi-\alpha_{(i+2)(i+3)}, \alpha_{(i+3)(i+4)}$	v_{614}: m_6-c_{14}
	$-\alpha_{i(i+1)}, -\pi+\alpha_{(i+1)(i+2)}, -\pi+\alpha_{(i+2)(i+3)}, \alpha_{(i+3)(i+4)}$	v_{615}: m_6-c_{15}
	$-\alpha_{i(i+1)}, -\pi+\alpha_{(i+1)(i+2)}, -\alpha_{(i+2)(i+3)}, -\pi+\alpha_{(i+3)(i+4)}$	v_{616}: m_6-c_{16}
m_7: $\pi-\theta_i$ $\longrightarrow$ $\pi+\theta_{(i+1)}$	$\pi-\alpha_{i(i+1)}, \alpha_{(i+1)(i+2)}, \alpha_{(i+2)(i+3)}, -\pi+\alpha_{(i+3)(i+4)}$	v_{71}: m_7-c_1
	$\pi-\alpha_{i(i+1)}, \alpha_{(i+1)(i+2)}, \pi-\alpha_{(i+2)(i+3)}, \alpha_{(i+3)(i+4)}$	v_{72}: m_7-c_2
	$\pi-\alpha_{i(i+1)}, \alpha_{(i+1)(i+2)}, -\pi+\alpha_{(i+2)(i+3)}, \alpha_{(i+3)(i+4)}$	v_{73}: m_7-c_3
	$\pi-\alpha_{i(i+1)}, \alpha_{(i+1)(i+2)}, -\alpha_{(i+2)(i+3)}, -\pi+\alpha_{(i+3)(i+4)}$	v_{74}: m_7-c_4
	$\pi-\alpha_{i(i+1)}, -\pi+\alpha_{(i+1)(i+2)}, \alpha_{(i+2)(i+3)}, \alpha_{(i+3)(i+4)}$	v_{75}: m_7-c_5
	$\pi-\alpha_{i(i+1)}, -\pi+\alpha_{(i+1)(i+2)}, \pi-\alpha_{(i+2)(i+3)}, -\pi+\alpha_{(i+3)(i+4)}$	v_{76}: m_7-c_6
	$\pi-\alpha_{i(i+1)}, -\pi+\alpha_{(i+1)(i+2)}, -\pi+\alpha_{(i+2)(i+3)}, -\pi+\alpha_{(i+3)(i+4)}$	v_{77}: m_7-c_7
	$\pi-\alpha_{i(i+1)}, -\pi+\alpha_{(i+1)(i+2)}, -\alpha_{(i+2)(i+3)}, \alpha_{(i+3)(i+4)}$	v_{78}: m_7-c_8
	$-\pi+\alpha_{i(i+1)}, \pi-\alpha_{(i+1)(i+2)}, \alpha_{(i+2)(i+3)}, -\alpha_{(i+3)(i+4)}$	v_{79}: m_7-c_9
	$-\pi+\alpha_{i(i+1)}, \pi-\alpha_{(i+1)(i+2)}, \pi-\alpha_{(i+2)(i+3)}, \pi-\alpha_{(i+3)(i+4)}$	v_{710}: m_7-c_{10}
	$-\pi+\alpha_{i(i+1)}, \pi-\alpha_{(i+1)(i+2)}, -\pi+\alpha_{(i+2)(i+3)}, \pi-\alpha_{(i+3)(i+4)}$	v_{711}: m_7-c_{11}
	$-\pi+\alpha_{i(i+1)}, \pi-\alpha_{(i+1)(i+2)}, -\alpha_{(i+2)(i+3)}, -\alpha_{(i+3)(i+4)}$	v_{712}: m_7-c_{12}
	$-\pi+\alpha_{i(i+1)}, -\alpha_{(i+1)(i+2)}, \alpha_{(i+2)(i+3)}, \pi-\alpha_{(i+3)(i+4)}$	v_{713}: m_7-c_{13}
	$-\pi+\alpha_{i(i+1)}, -\alpha_{(i+1)(i+2)}, \pi-\alpha_{(i+2)(i+3)}, -\alpha_{(i+3)(i+4)}$	v_{714}: m_7-c_{14}
	$-\pi+\alpha_{i(i+1)}, -\alpha_{(i+1)(i+2)}, -\pi+\alpha_{(i+2)(i+3)}, -\alpha_{(i+3)(i+4)}$	v_{715}: m_7-c_{15}
	$-\pi+\alpha_{i(i+1)}, -\alpha_{(i+1)(i+2)}, -\alpha_{(i+2)(i+3)}, \pi-\alpha_{(i+3)(i+4)}$	v_{716}: m_7-c_{16}
m_8: $\pi-\theta_i$ $\longrightarrow$ $-\theta_{(i+1)}$	$\alpha_{i(i+1)}, \alpha_{(i+1)(i+2)}, \alpha_{(i+2)(i+3)}, -\alpha_{(i+3)(i+4)}$	v_{81}: m_8-c_1
	$\alpha_{i(i+1)}, \alpha_{(i+1)(i+2)}, \pi-\alpha_{(i+2)(i+3)}, \pi-\alpha_{(i+3)(i+4)}$	v_{82}: m_8-c_2
	$\alpha_{i(i+1)}, \alpha_{(i+1)(i+2)}, -\pi+\alpha_{(i+2)(i+3)}, \pi-\alpha_{(i+3)(i+4)}$	v_{83}: m_8-c_3
	$\alpha_{i(i+1)}, \alpha_{(i+1)(i+2)}, -\alpha_{(i+2)(i+3)}, -\alpha_{(i+3)(i+4)}$	v_{84}: m_8-c_4
	$\alpha_{i(i+1)}, -\pi+\alpha_{(i+1)(i+2)}, \alpha_{(i+2)(i+3)}, \pi-\alpha_{(i+3)(i+4)}$	v_{85}: m_8-c_5
	$\alpha_{i(i+1)}, -\pi+\alpha_{(i+1)(i+2)}, \pi-\alpha_{(i+2)(i+3)}, -\alpha_{(i+3)(i+4)}$	v_{86}: m_8-c_6
	$\alpha_{i(i+1)}, -\pi+\alpha_{(i+1)(i+2)}, -\pi+\alpha_{(i+2)(i+3)}, -\alpha_{(i+3)(i+4)}$	v_{87}: m_8-c_7
	$\alpha_{i(i+1)}, -\pi+\alpha_{(i+1)(i+2)}, -\alpha_{(i+2)(i+3)}, \pi-\alpha_{(i+3)(i+4)}$	v_{88}: m_8-c_8
	$-\alpha_{i(i+1)}, \pi-\alpha_{(i+1)(i+2)}, \alpha_{(i+2)(i+3)}, -\pi+\alpha_{(i+3)(i+4)}$	v_{89}: m_8-c_9

	$-\alpha_{i(i+1)}, \pi-\alpha_{(i+1)(i+2)}, \pi-\alpha_{(i+2)(i+3)}, \alpha_{(i+3)(i+4)}$	v_{810}: m_8-c_{10}
	$-\alpha_{i(i+1)}, \pi-\alpha_{(i+1)(i+2)}, -\pi+\alpha_{(i+2)(i+3)}, \alpha_{(i+3)(i+4)}$	v_{811}: m_8-c_{11}
	$-\alpha_{i(i+1)}, \pi-\alpha_{(i+1)(i+2)}, -\alpha_{(i+2)(i+3)}, -\pi+\alpha_{(i+3)(i+4)}$	v_{812}: m_8-c_{12}
	$-\alpha_{i(i+1)}, -\alpha_{(i+1)(i+2)}, \alpha_{(i+2)(i+3)}, \alpha_{(i+3)(i+4)}$	v_{813}: m_8-c_{13}
	$-\alpha_{i(i+1)}, -\alpha_{(i+1)(i+2)}, \pi-\alpha_{(i+2)(i+3)}, -\pi+\alpha_{(i+3)(i+4)}$	v_{814}: m_8-c_{14}
	$-\alpha_{i(i+1)}, -\alpha_{(i+1)(i+2)}, -\pi+\alpha_{(i+2)(i+3)}, -\pi+\alpha_{(i+3)(i+4)}$	v_{815}: m_8-c_{15}
	$-\alpha_{i(i+1)}, -\alpha_{(i+1)(i+2)}, -\alpha_{(i+2)(i+3)}, \alpha_{(i+3)(i+4)}$	v_{816}: m_8-c_{16}

Table A2 (1) Variants for double-plane symmetric case ($\alpha_{i(i+1)} \in (0, \pi)$)

Variant types	v_{t1}	v_{t2}
Types of the four spherical 4R linkages	$\alpha_{12}^a = \pi - \alpha_{12}, \alpha_{12}^b = \pi - \alpha_{12}, \alpha_{12}^c = \alpha_{12}, \alpha_{12}^d = \alpha_{12},$ $\alpha_{23}^a = \alpha_{23}, \alpha_{23}^b = \alpha_{23}, \alpha_{23}^c = \alpha_{23}, \alpha_{23}^d = \alpha_{23},$ $\alpha_{34}^a = \alpha_{34}, \alpha_{34}^b = \alpha_{34}, \alpha_{34}^c = \alpha_{34}, \alpha_{34}^d = \alpha_{34},$ $\alpha_{41}^a = \pi - \alpha_{41}, \alpha_{41}^b = \pi - \alpha_{41}, \alpha_{41}^c = \alpha_{41}, \alpha_{41}^d = \alpha_{41}.$	$\alpha_{12}^a = \alpha_{12}, \alpha_{12}^b = \alpha_{12}, \alpha_{12}^c = \alpha_{12}, \alpha_{12}^d = \alpha_{12},$ $\alpha_{23}^a = \pi - \alpha_{23}, \alpha_{23}^b = \pi - \alpha_{23}, \alpha_{23}^c = \alpha_{23}, \alpha_{23}^d = \alpha_{23},$ $\alpha_{34}^a = \pi - \alpha_{34}, \alpha_{34}^b = \pi - \alpha_{34}, \alpha_{34}^c = \alpha_{34}, \alpha_{34}^d = \alpha_{34},$ $\alpha_{41}^a = \alpha_{41}, \alpha_{41}^b = \alpha_{41}, \alpha_{41}^c = \alpha_{41}, \alpha_{41}^d = \alpha_{41}.$
Variant types	v_{t3}	v_{t4}
Types of the four spherical 4R linkages	$\alpha_{12}^a = \pi - \alpha_{12}, \alpha_{12}^b = \pi - \alpha_{12}, \alpha_{12}^c = \alpha_{12}, \alpha_{12}^d = \alpha_{12},$ $\alpha_{23}^a = \pi - \alpha_{23}, \alpha_{23}^b = \pi - \alpha_{23}, \alpha_{23}^c = \alpha_{23}, \alpha_{23}^d = \alpha_{23},$ $\alpha_{34}^a = \pi - \alpha_{34}, \alpha_{34}^b = \pi - \alpha_{34}, \alpha_{34}^c = \alpha_{34}, \alpha_{34}^d = \alpha_{34},$ $\alpha_{41}^a = \pi - \alpha_{41}, \alpha_{41}^b = \pi - \alpha_{41}, \alpha_{41}^c = \alpha_{41}, \alpha_{41}^d = \alpha_{41}.$	$\alpha_{12}^a = \alpha_{12}, \alpha_{12}^b = \pi - \alpha_{12}, \alpha_{12}^c = \pi - \alpha_{12}, \alpha_{12}^d = \alpha_{12},$ $\alpha_{23}^a = \alpha_{23}, \alpha_{23}^b = \pi - \alpha_{23}, \alpha_{23}^c = \pi - \alpha_{23}, \alpha_{23}^d = \alpha_{23},$ $\alpha_{34}^a = \alpha_{34}, \alpha_{34}^b = \alpha_{34}, \alpha_{34}^c = \alpha_{34}, \alpha_{34}^d = \alpha_{34},$ $\alpha_{41}^a = \alpha_{41}, \alpha_{41}^b = \alpha_{41}, \alpha_{41}^c = \alpha_{41}, \alpha_{41}^d = \alpha_{41}.$
Variant types	v_{t5}	v_{t6}
Types of the four spherical 4R linkages	$\alpha_{12}^a = \alpha_{12}, \alpha_{12}^b = \pi - \alpha_{12}, \alpha_{12}^c = \pi - \alpha_{12}, \alpha_{12}^d = \alpha_{12},$ $\alpha_{23}^a = \alpha_{23}, \alpha_{23}^b = \pi - \alpha_{23}, \alpha_{23}^c = \pi - \alpha_{23}, \alpha_{23}^d = \alpha_{23},$ $\alpha_{34}^a = \alpha_{34}, \alpha_{34}^b = \pi - \alpha_{34}, \alpha_{34}^c = \pi - \alpha_{34}, \alpha_{34}^d = \alpha_{34},$ $\alpha_{41}^a = \alpha_{41}, \alpha_{41}^b = \pi - \alpha_{41}, \alpha_{41}^c = \pi - \alpha_{41}, \alpha_{41}^d = \alpha_{41}.$	$\alpha_{12}^a = \alpha_{12}, \alpha_{12}^b = \alpha_{12}, \alpha_{12}^c = \alpha_{12}, \alpha_{12}^d = \alpha_{12},$ $\alpha_{23}^a = \alpha_{23}, \alpha_{23}^b = \alpha_{23}, \alpha_{23}^c = \alpha_{23}, \alpha_{23}^d = \alpha_{23},$ $\alpha_{34}^a = \alpha_{34}, \alpha_{34}^b = \pi - \alpha_{34}, \alpha_{34}^c = \pi - \alpha_{34}, \alpha_{34}^d = \alpha_{34},$ $\alpha_{41}^a = \alpha_{41}, \alpha_{41}^b = \pi - \alpha_{41}, \alpha_{41}^c = \pi - \alpha_{41}, \alpha_{41}^d = \alpha_{41}.$
Variant types	v_{t7}	v_{t8}
Types of the four spherical 4R linkages	$\alpha_{12}^a = \pi - \alpha_{12}, \alpha_{12}^b = \alpha_{12}, \alpha_{12}^c = \pi - \alpha_{12}, \alpha_{12}^d = \alpha_{12},$ $\alpha_{23}^a = \alpha_{23}, \alpha_{23}^b = \pi - \alpha_{23}, \alpha_{23}^c = \pi - \alpha_{23}, \alpha_{23}^d = \alpha_{23},$ $\alpha_{34}^a = \alpha_{34}, \alpha_{34}^b = \alpha_{34}, \alpha_{34}^c = \alpha_{34}, \alpha_{34}^d = \alpha_{34},$ $\alpha_{41}^a = \pi - \alpha_{41}, \alpha_{41}^b = \pi - \alpha_{41}, \alpha_{41}^c = \alpha_{41}, \alpha_{41}^d = \alpha_{41}.$	$\alpha_{12}^a = \pi - \alpha_{12}, \alpha_{12}^b = \pi - \alpha_{12}, \alpha_{12}^c = \alpha_{12}, \alpha_{12}^d = \alpha_{12},$ $\alpha_{23}^a = \alpha_{23}, \alpha_{23}^b = \alpha_{23}, \alpha_{23}^c = \alpha_{23}, \alpha_{23}^d = \alpha_{23},$ $\alpha_{34}^a = \alpha_{34}, \alpha_{34}^b = \pi - \alpha_{34}, \alpha_{34}^c = \pi - \alpha_{34}, \alpha_{34}^d = \alpha_{34},$ $\alpha_{41}^a = \pi - \alpha_{41}, \alpha_{41}^b = \alpha_{41}, \alpha_{41}^c = \pi - \alpha_{41}, \alpha_{41}^d = \alpha_{41}.$
Variant types	v_{t9}	v_{t10}
Types of the four spherical 4R linkages	$\alpha_{12}^a = \pi - \alpha_{12}, \alpha_{12}^b = \alpha_{12}, \alpha_{12}^c = \pi - \alpha_{12}, \alpha_{12}^d = \alpha_{12},$ $\alpha_{23}^a = \alpha_{23}, \alpha_{23}^b = \pi - \alpha_{23}, \alpha_{23}^c = \pi - \alpha_{23}, \alpha_{23}^d = \alpha_{23},$ $\alpha_{34}^a = \alpha_{34}, \alpha_{34}^b = \alpha_{34}, \alpha_{34}^c = \pi - \alpha_{34}, \alpha_{34}^d = \alpha_{34},$ $\alpha_{41}^a = \pi - \alpha_{41}, \alpha_{41}^b = \pi - \alpha_{41}, \alpha_{41}^c = \pi - \alpha_{41}, \alpha_{41}^d = \alpha_{41}$	$\alpha_{12}^a = \alpha_{12}, \alpha_{12}^b = \pi - \alpha_{12}, \alpha_{12}^c = \pi - \alpha_{12}, \alpha_{12}^d = \alpha_{12},$ $\alpha_{23}^a = \pi - \alpha_{23}, \alpha_{23}^b = \alpha_{23}, \alpha_{23}^c = \pi - \alpha_{23}, \alpha_{23}^d = \alpha_{23},$ $\alpha_{34}^a = \pi - \alpha_{34}, \alpha_{34}^b = \pi - \alpha_{34}, \alpha_{34}^c = \alpha_{34}, \alpha_{34}^d = \alpha_{34},$ $\alpha_{41}^a = \alpha_{41}, \alpha_{41}^b = \alpha_{41}, \alpha_{41}^c = \alpha_{41}, \alpha_{41}^d = \alpha_{41}.$
Variant types	v_{t11}	v_{t12}
Types of the four spherical 4R linkages	$\alpha_{12}^a = \alpha_{12}, \alpha_{12}^b = \pi - \alpha_{12}, \alpha_{12}^c = \pi - \alpha_{12}, \alpha_{12}^d = \alpha_{12},$ $\alpha_{23}^a = \pi - \alpha_{23}, \alpha_{23}^b = \alpha_{23}, \alpha_{23}^c = \pi - \alpha_{23}, \alpha_{23}^d = \alpha_{23},$ $\alpha_{34}^a = \pi - \alpha_{34}, \alpha_{34}^b = \alpha_{34}, \alpha_{34}^c = \pi - \alpha_{34}, \alpha_{34}^d = \alpha_{34},$ $\alpha_{41}^a = \alpha_{41}, \alpha_{41}^b = \pi - \alpha_{41}, \alpha_{41}^c = \pi - \alpha_{41}, \alpha_{41}^d = \alpha_{41}.$	$\alpha_{12}^a = \alpha_{12}, \alpha_{12}^b = \alpha_{12}, \alpha_{12}^c = \alpha_{12}, \alpha_{12}^d = \alpha_{12},$ $\alpha_{23}^a = \pi - \alpha_{23}, \alpha_{23}^b = \pi - \alpha_{23}, \alpha_{23}^c = \alpha_{23}, \alpha_{23}^d = \alpha_{23},$ $\alpha_{34}^a = \pi - \alpha_{34}, \alpha_{34}^b = \alpha_{34}, \alpha_{34}^c = \pi - \alpha_{34}, \alpha_{34}^d = \alpha_{34},$ $\alpha_{41}^a = \alpha_{41}, \alpha_{41}^b = \pi - \alpha_{41}, \alpha_{41}^c = \pi - \alpha_{41}, \alpha_{41}^d = \alpha_{41}.$

Variant types	v_{t13}	v_{t14}
Types of the four spherical 4R linkages	$\alpha_{12}^a=\pi-\alpha_{12},\alpha_{12}^b=\alpha_{12},\alpha_{12}^c=\pi-\alpha_{12},\alpha_{12}^d=\alpha_{12},$ $\alpha_{23}^a=\pi-\alpha_{23},\alpha_{23}^b=\alpha_{23},\alpha_{23}^c=\pi-\alpha_{23},\alpha_{23}^d=\alpha_{23},$ $\alpha_{34}^a=\pi-\alpha_{34},\alpha_{34}^b=\pi-\alpha_{34},\alpha_{34}^c=\alpha_{34},\alpha_{34}^d=\alpha_{34},$ $\alpha_{41}^a=\pi-\alpha_{41},\alpha_{41}^b=\pi-\alpha_{41},\alpha_{41}^c=\alpha_{41},\alpha_{41}^d=\alpha_{41}.$	$\alpha_{12}^a=\pi-\alpha_{12},\alpha_{12}^b=\alpha_{12},\alpha_{12}^c=\pi-\alpha_{12},\alpha_{12}^d=\alpha_{12},$ $\alpha_{23}^a=\pi-\alpha_{23},\alpha_{23}^b=\alpha_{23},\alpha_{23}^c=\pi-\alpha_{23},\alpha_{23}^d=\alpha_{23},$ $\alpha_{34}^a=\pi-\alpha_{34},\alpha_{34}^b=\alpha_{34},\alpha_{34}^c=\pi-\alpha_{34},\alpha_{34}^d=\alpha_{34},$ $\alpha_{41}^a=\pi-\alpha_{41},\alpha_{41}^b=\alpha_{41},\alpha_{41}^c=\pi-\alpha_{41},\alpha_{41}^d=\alpha_{41}.$

Variant types	v_{t15}
Types of the four spherical 4R linkages	$\alpha_{12}^a=\pi-\alpha_{12},\alpha_{12}^b=\pi-\alpha_{12},\alpha_{12}^c=\alpha_{12},\alpha_{12}^d=\alpha_{12},$ $\alpha_{23}^a=\pi-\alpha_{23},\alpha_{23}^b=\pi-\alpha_{23},\alpha_{23}^c=\alpha_{23},\alpha_{23}^d=\alpha_{23},$ $\alpha_{34}^a=\pi-\alpha_{34},\alpha_{34}^b=\alpha_{34},\alpha_{34}^c=\pi-\alpha_{34},\alpha_{34}^d=\alpha_{34},$ $\alpha_{41}^a=\pi-\alpha_{41},\alpha_{41}^b=\alpha_{41},\alpha_{41}^c=\pi-\alpha_{41},\alpha_{41}^d=\alpha_{41}.$

Table A2 (2) Variants for plane symmetric case ($\alpha_{i(i+1)} \in (0, \pi)$)

Variant types	v_{s1}	v_{s2}
Types of the four spherical 4R linkages	$\alpha_{12}^a = \alpha_{12}, \alpha_{12}^b = \pi - \alpha_{12}, \alpha_{12}^c = \pi - \alpha_{12}, \alpha_{12}^d = \alpha_{12},$ $\alpha_{23}^a = \alpha_{23}, \alpha_{23}^b = \pi - \alpha_{23}, \alpha_{23}^c = \pi - \alpha_{23}, \alpha_{23}^d = \alpha_{23},$ $\alpha_{34}^a = \alpha_{34}, \alpha_{34}^b = \alpha_{34}, \alpha_{34}^c = \alpha_{34}, \alpha_{34}^d = \alpha_{34},$ $\alpha_{41}^a = \alpha_{41}, \alpha_{41}^b = \alpha_{41}, \alpha_{41}^c = \alpha_{41}, \alpha_{41}^d = \alpha_{41}.$	$\alpha_{12}^a = \alpha_{12}, \alpha_{12}^b = \alpha_{12}, \alpha_{12}^c = \alpha_{12}, \alpha_{12}^d = \alpha_{12},$ $\alpha_{23}^a = \alpha_{23}, \alpha_{23}^b = \alpha_{23}, \alpha_{23}^c = \alpha_{23}, \alpha_{23}^d = \alpha_{23},$ $\alpha_{34}^a = \alpha_{34}, \alpha_{34}^b = \pi - \alpha_{34}, \alpha_{34}^c = \pi - \alpha_{34}, \alpha_{34}^d = \alpha_{34},$ $\alpha_{41}^a = \alpha_{41}, \alpha_{41}^b = \pi - \alpha_{41}, \alpha_{41}^c = \pi - \alpha_{41}, \alpha_{41}^d = \alpha_{41}.$
Variant types	v_{s3}	v_{s4}
Types of the four spherical 4R linkages	$\alpha_{12}^a = \alpha_{12}, \alpha_{12}^b = \alpha_{12}, \alpha_{12}^c = \pi - \alpha_{12}, \alpha_{12}^d = \pi - \alpha_{12},$ $\alpha_{23}^a = \alpha_{23}, \alpha_{23}^b = \alpha_{23}, \alpha_{23}^c = \pi - \alpha_{23}, \alpha_{23}^d = \pi - \alpha_{23},$ $\alpha_{34}^a = \alpha_{34}, \alpha_{34}^b = \alpha_{34}, \alpha_{34}^c = \pi - \alpha_{34}, \alpha_{34}^d = \pi - \alpha_{34},$ $\alpha_{41}^a = \alpha_{41}, \alpha_{41}^b = \alpha_{41}, \alpha_{41}^c = \pi - \alpha_{41}, \alpha_{41}^d = \pi - \alpha_{41}.$	$\alpha_{12}^a = \pi - \alpha_{12}, \alpha_{12}^b = \alpha_{12}, \alpha_{12}^c = \alpha_{12}, \alpha_{12}^d = \alpha_{12},$ $\alpha_{23}^a = \alpha_{23}, \alpha_{23}^b = \pi - \alpha_{23}, \alpha_{23}^c = \alpha_{23}, \alpha_{23}^d = \alpha_{23},$ $\alpha_{34}^a = \alpha_{34}, \alpha_{34}^b = \pi - \alpha_{34}, \alpha_{34}^c = \alpha_{34}, \alpha_{34}^d = \alpha_{34},$ $\alpha_{41}^a = \pi - \alpha_{41}, \alpha_{41}^b = \alpha_{41}, \alpha_{41}^c = \alpha_{41}, \alpha_{41}^d = \alpha_{41}.$
Variant types	v_{s5}	v_{s6}
Types of the four spherical 4R linkages	$\alpha_{12}^a = \alpha_{12}, \alpha_{12}^b = \pi - \alpha_{12}, \alpha_{12}^c = \alpha_{12}, \alpha_{12}^d = \alpha_{12},$ $\alpha_{23}^a = \pi - \alpha_{23}, \alpha_{23}^b = \alpha_{23}, \alpha_{23}^c = \alpha_{23}, \alpha_{23}^d = \alpha_{23},$ $\alpha_{34}^a = \pi - \alpha_{34}, \alpha_{34}^b = \alpha_{34}, \alpha_{34}^c = \alpha_{34}, \alpha_{34}^d = \alpha_{34},$ $\alpha_{41}^a = \alpha_{41}, \alpha_{41}^b = \pi - \alpha_{41}, \alpha_{41}^c = \alpha_{41}, \alpha_{41}^d = \alpha_{41}.$	$\alpha_{12}^a = \pi - \alpha_{12}, \alpha_{12}^b = \pi - \alpha_{12}, \alpha_{12}^c = \alpha_{12}, \alpha_{12}^d = \alpha_{12},$ $\alpha_{23}^a = \pi - \alpha_{23}, \alpha_{23}^b = \pi - \alpha_{23}, \alpha_{23}^c = \alpha_{23}, \alpha_{23}^d = \alpha_{23},$ $\alpha_{34}^a = \pi - \alpha_{34}, \alpha_{34}^b = \pi - \alpha_{34}, \alpha_{34}^c = \alpha_{34}, \alpha_{34}^d = \alpha_{34},$ $\alpha_{41}^a = \pi - \alpha_{41}, \alpha_{41}^b = \pi - \alpha_{41}, \alpha_{41}^c = \alpha_{41}, \alpha_{41}^d = \alpha_{41}.$
Variant types	v_{s7}	v_{s8}
Types of the four spherical 4R linkages	$\alpha_{12}^a = \pi - \alpha_{12}, \alpha_{12}^b = \pi - \alpha_{12}, \alpha_{12}^c = \pi - \alpha_{12}, \alpha_{12}^d = \alpha_{12},$ $\alpha_{23}^a = \alpha_{23}, \alpha_{23}^b = \alpha_{23}, \alpha_{23}^c = \pi - \alpha_{23}, \alpha_{23}^d = \alpha_{23},$ $\alpha_{34}^a = \alpha_{34}, \alpha_{34}^b = \pi - \alpha_{34}, \alpha_{34}^c = \alpha_{34}, \alpha_{34}^d = \alpha_{34},$ $\alpha_{41}^a = \pi - \alpha_{41}, \alpha_{41}^b = \alpha_{41}, \alpha_{41}^c = \alpha_{41}, \alpha_{41}^d = \alpha_{41}.$	$\alpha_{12}^a = \pi - \alpha_{12}, \alpha_{12}^b = \alpha_{12}, \alpha_{12}^c = \alpha_{12}, \alpha_{12}^d = \alpha_{12},$ $\alpha_{23}^a = \alpha_{23}, \alpha_{23}^b = \pi - \alpha_{23}, \alpha_{23}^c = \alpha_{23}, \alpha_{23}^d = \alpha_{23},$ $\alpha_{34}^a = \alpha_{34}, \alpha_{34}^b = \alpha_{34}, \alpha_{34}^c = \pi - \alpha_{34}, \alpha_{34}^d = \alpha_{34},$ $\alpha_{41}^a = \pi - \alpha_{41}, \alpha_{41}^b = \pi - \alpha_{41}, \alpha_{41}^c = \pi - \alpha_{41}, \alpha_{41}^d = \alpha_{41}.$
Variant types	v_{s9}	v_{s10}
Types of the four spherical 4R linkages	$\alpha_{12}^a = \pi - \alpha_{12}, \alpha_{12}^b = \pi - \alpha_{12}, \alpha_{12}^c = \pi - \alpha_{12}, \alpha_{12}^d = \alpha_{12},$ $\alpha_{23}^a = \alpha_{23}, \alpha_{23}^b = \alpha_{23}, \alpha_{23}^c = \pi - \alpha_{23}, \alpha_{23}^d = \alpha_{23},$ $\alpha_{34}^a = \alpha_{34}, \alpha_{34}^b = \alpha_{34}, \alpha_{34}^c = \pi - \alpha_{34}, \alpha_{34}^d = \alpha_{34},$ $\alpha_{41}^a = \pi - \alpha_{41}, \alpha_{41}^b = \pi - \alpha_{41}, \alpha_{41}^c = \pi - \alpha_{41}, \alpha_{41}^d = \alpha_{41}.$	$\alpha_{12}^a = \alpha_{12}, \alpha_{12}^b = \alpha_{12}, \alpha_{12}^c = \pi - \alpha_{12}, \alpha_{12}^d = \alpha_{12},$ $\alpha_{23}^a = \pi - \alpha_{23}, \alpha_{23}^b = \pi - \alpha_{23}, \alpha_{23}^c = \pi - \alpha_{23}, \alpha_{23}^d = \alpha_{23},$ $\alpha_{34}^a = \pi - \alpha_{34}, \alpha_{34}^b = \alpha_{34}, \alpha_{34}^c = \alpha_{34}, \alpha_{34}^d = \alpha_{34},$ $\alpha_{41}^a = \alpha_{41}, \alpha_{41}^b = \pi - \alpha_{41}, \alpha_{41}^c = \alpha_{41}, \alpha_{41}^d = \alpha_{41}.$
Variant types	v_{s11}	v_{s12}
Types of the four spherical 4R linkages	$\alpha_{12}^a = \alpha_{12}, \alpha_{12}^b = \pi - \alpha_{12}, \alpha_{12}^c = \alpha_{12}, \alpha_{12}^d = \alpha_{12},$ $\alpha_{23}^a = \pi - \alpha_{23}, \alpha_{23}^b = \alpha_{23}, \alpha_{23}^c = \alpha_{23}, \alpha_{23}^d = \alpha_{23},$ $\alpha_{34}^a = \pi - \alpha_{34}, \alpha_{34}^b = \pi - \alpha_{34}, \alpha_{34}^c = \pi - \alpha_{34}, \alpha_{34}^d = \alpha_{34},$ $\alpha_{41}^a = \alpha_{41}, \alpha_{41}^b = \alpha_{41}, \alpha_{41}^c = \pi - \alpha_{41}, \alpha_{41}^d = \alpha_{41}.$	$\alpha_{12}^a = \alpha_{12}, \alpha_{12}^b = \alpha_{12}, \alpha_{12}^c = \pi - \alpha_{12}, \alpha_{12}^d = \alpha_{12},$ $\alpha_{23}^a = \pi - \alpha_{23}, \alpha_{23}^b = \pi - \alpha_{23}, \alpha_{23}^c = \pi - \alpha_{23}, \alpha_{23}^d = \alpha_{23},$ $\alpha_{34}^a = \pi - \alpha_{34}, \alpha_{34}^b = \pi - \alpha_{34}, \alpha_{34}^c = \pi - \alpha_{34}, \alpha_{34}^d = \alpha_{34},$ $\alpha_{41}^a = \alpha_{41}, \alpha_{41}^b = \alpha_{41}, \alpha_{41}^c = \pi - \alpha_{41}, \alpha_{41}^d = \alpha_{41}.$

Variant types	v_{s13}	v_{s14}
Types of the four spherical 4R linkages	$\alpha_{12}^a=\pi-\alpha_{12},\alpha_{12}^b=\alpha_{12},\alpha_{12}^c=\pi-\alpha_{12},\alpha_{12}^d=\alpha_{12},$ $\alpha_{23}^a=\pi-\alpha_{23},\alpha_{23}^b=\alpha_{23},\alpha_{23}^c=\pi-\alpha_{23},\alpha_{23}^d=\alpha_{23},$ $\alpha_{34}^a=\pi-\alpha_{34},\alpha_{34}^b=\pi-\alpha_{34},\alpha_{34}^c=\alpha_{34},\alpha_{34}^d=\alpha_{34},$ $\alpha_{41}^a=\pi-\alpha_{41},\alpha_{41}^b=\pi-\alpha_{41},\alpha_{41}^c=\alpha_{41},\alpha_{41}^d=\alpha_{41}.$	$\alpha_{12}^a=\pi-\alpha_{12},\alpha_{12}^b=\pi-\alpha_{12},\alpha_{12}^c=\alpha_{12},\alpha_{12}^d=\alpha_{12},$ $\alpha_{23}^a=\pi-\alpha_{23},\alpha_{23}^b=\pi-\alpha_{23},\alpha_{23}^c=\alpha_{23},\alpha_{23}^d=\alpha_{23},$ $\alpha_{34}^a=\pi-\alpha_{34},\alpha_{34}^b=\alpha_{34},\alpha_{34}^c=\pi-\alpha_{34},\alpha_{34}^d=\alpha_{34},$ $\alpha_{41}^a=\pi-\alpha_{41},\alpha_{41}^b=\alpha_{41},\alpha_{41}^c=\pi-\alpha_{41},\alpha_{41}^d=\alpha_{41}.$

Variant types	v_{s15}
Types of the four spherical 4R linkages	$\alpha_{12}^a=\pi-\alpha_{12},\alpha_{12}^b=\alpha_{12},\alpha_{12}^c=\pi-\alpha_{12},\alpha_{12}^d=\alpha_{12},$ $\alpha_{23}^a=\pi-\alpha_{23},\alpha_{23}^b=\alpha_{23},\alpha_{23}^c=\pi-\alpha_{23},\alpha_{23}^d=\alpha_{23},$ $\alpha_{34}^a=\pi-\alpha_{34},\alpha_{34}^b=\alpha_{34},\alpha_{34}^c=\pi-\alpha_{34},\alpha_{34}^d=\alpha_{34},$ $\alpha_{41}^a=\pi-\alpha_{41},\alpha_{41}^b=\alpha_{41},\alpha_{41}^c=\pi-\alpha_{41},\alpha_{41}^d=\alpha_{41}.$

Table A2 (3) Variants for rotational case ($\alpha_{i(i+1)} \in (0, \pi)$)

Variant types	v_{r1}	v_{r2}
Types of the four spherical 4R linkages	$\alpha_{12}^a = \pi - \alpha_{12}, \alpha_{12}^b = \alpha_{12}, \alpha_{12}^c = \alpha_{12}, = \alpha_{12}^d = \alpha_{12},$ $\alpha_{23}^a = \alpha_{23}, \alpha_{23}^b = \pi - \alpha_{23}, \alpha_{23}^c = \alpha_{23}, \alpha_{23}^d = \alpha_{23},$ $\alpha_{34}^a = \alpha_{34}, \alpha_{34}^b = \pi - \alpha_{34}, \alpha_{34}^c = \alpha_{34}, \alpha_{34}^d = \alpha_{34},$ $\alpha_{41}^a = \pi - \alpha_{41}, \alpha_{41}^b = \alpha_{41}, \alpha_{41}^c = \alpha_{41}, \alpha_{41}^d = \alpha_{41}.$	$\alpha_{12}^a = \alpha_{12}, \alpha_{12}^b = \pi - \alpha_{12}, \alpha_{12}^c = \alpha_{12}, \alpha_{12}^d = \alpha_{12},$ $\alpha_{23}^a = \pi - \alpha_{23}, \alpha_{23}^b = \alpha_{23}, \alpha_{23}^c = \alpha_{23}, \alpha_{23}^d = \alpha_{23},$ $\alpha_{34}^a = \pi - \alpha_{34}, \alpha_{34}^b = \alpha_{34}, \alpha_{34}^c = \alpha_{34}, \alpha_{34}^d = \alpha_{34},$ $\alpha_{41}^a = \alpha_{41}, \alpha_{41}^b = \pi - \alpha_{41}, \alpha_{41}^c = \alpha_{41}, \alpha_{41}^d = \alpha_{41}.$
Variant types	v_{r3}	v_{r4}
Types of the four spherical 4R linkages	$\alpha_{12}^a = \pi - \alpha_{12}, \alpha_{12}^b = \pi - \alpha_{12}, \alpha_{12}^c = \alpha_{12}, \alpha_{12}^d = \alpha_{12},$ $\alpha_{23}^a = \pi - \alpha_{23}, \alpha_{23}^b = \pi - \alpha_{23}, \alpha_{23}^c = \alpha_{23}, \alpha_{23}^d = \alpha_{23},$ $\alpha_{34}^a = \pi - \alpha_{34}, \alpha_{34}^b = \pi - \alpha_{34}, \alpha_{34}^c = \alpha_{34}, \alpha_{34}^d = \alpha_{34},$ $\alpha_{41}^a = \pi - \alpha_{41}, \alpha_{41}^b = \pi - \alpha_{41}, \alpha_{41}^c = \alpha_{41}, \alpha_{41}^d = \alpha_{41}.$	$\alpha_{12}^a = \pi - \alpha_{12}, \alpha_{12}^b = \pi - \alpha_{12}, \alpha_{12}^c = \alpha_{12}, \alpha_{12}^d = \alpha_{12},$ $\alpha_{23}^a = \alpha_{23}, \alpha_{23}^b = \alpha_{23}, \alpha_{23}^c = \alpha_{23}, \alpha_{23}^d = \alpha_{23},$ $\alpha_{34}^a = \alpha_{34}, \alpha_{34}^b = \pi - \alpha_{34}, \alpha_{34}^c = \pi - \alpha_{34}, \alpha_{34}^d = \alpha_{34},$ $\alpha_{41}^a = \pi - \alpha_{41}, \alpha_{41}^b = \alpha_{41}, \alpha_{41}^c = \pi - \alpha_{41}, \alpha_{41}^d = \alpha_{41}.$
Variant types	v_{r5}	v_{r6}
Types of the four spherical 4R linkages	$\alpha_{12}^a = \pi - \alpha_{12}, \alpha_{12}^b = \alpha_{12}, \alpha_{12}^c = \pi - \alpha_{12}, \alpha_{12}^d = \alpha_{12},$ $\alpha_{23}^a = \alpha_{23}, \alpha_{23}^b = \pi - \alpha_{23}, \alpha_{23}^c = \pi - \alpha_{23}, \alpha_{23}^d = \alpha_{23},$ $\alpha_{34}^a = \alpha_{34}, \alpha_{34}^b = \alpha_{34}, \alpha_{34}^c = \alpha_{34}, \alpha_{34}^d = \alpha_{34},$ $\alpha_{41}^a = \pi - \alpha_{41}, \alpha_{41}^b = \pi - \alpha_{41}, \alpha_{41}^c = \alpha_{41}, \alpha_{41}^d = \alpha_{41}.$	$\alpha_{12}^a = \pi - \alpha_{12}, \alpha_{12}^b = \pi - \alpha_{12}, \alpha_{12}^c = \pi - \alpha_{12}, \alpha_{12}^d = \alpha_{12},$ $\alpha_{23}^a = \alpha_{23}, \alpha_{23}^b = \alpha_{23}, \alpha_{23}^c = \pi - \alpha_{23}, \alpha_{23}^d = \alpha_{23},$ $\alpha_{34}^a = \alpha_{34}, \alpha_{34}^b = \alpha_{34}, \alpha_{34}^c = \pi - \alpha_{34}, \alpha_{34}^d = \alpha_{34},$ $\alpha_{41}^a = \pi - \alpha_{41}, \alpha_{41}^b = \pi - \alpha_{41}, \alpha_{41}^c = \pi - \alpha_{41}, \alpha_{41}^d = \alpha_{41}.$
Variant types	v_{r7}	v_{r8}
Types of the four spherical 4R linkages	$\alpha_{12}^a = \alpha_{12}, \alpha_{12}^b = \alpha_{12}, \alpha_{12}^c = \alpha_{12}, \alpha_{12}^d = \alpha_{12},$ $\alpha_{23}^a = \pi - \alpha_{23}, \alpha_{23}^b = \pi - \alpha_{23}, \alpha_{23}^c = \alpha_{23}, \alpha_{23}^d = \alpha_{23},$ $\alpha_{34}^a = \pi - \alpha_{34}, \alpha_{34}^b = \alpha_{34}, \alpha_{34}^c = \pi - \alpha_{34}, \alpha_{34}^d = \alpha_{34},$ $\alpha_{41}^a = \alpha_{41}, \alpha_{41}^b = \pi - \alpha_{41}, \alpha_{41}^c = \pi - \alpha_{41}, \alpha_{41}^d = \alpha_{41}.$	$\alpha_{12}^a = \alpha_{12}, \alpha_{12}^b = \pi - \alpha_{12}, \alpha_{12}^c = \pi - \alpha_{12}, \alpha_{12}^d = \alpha_{12},$ $\alpha_{23}^a = \pi - \alpha_{23}, \alpha_{23}^b = \alpha_{23}, \alpha_{23}^c = \pi - \alpha_{23}, \alpha_{23}^d = \alpha_{23},$ $\alpha_{34}^a = \pi - \alpha_{34}, \alpha_{34}^b = \pi - \alpha_{34}, \alpha_{34}^c = \alpha_{34}, \alpha_{34}^d = \alpha_{34},$ $\alpha_{41}^a = \alpha_{41}, \alpha_{41}^b = \alpha_{41}, \alpha_{41}^c = \alpha_{41}, \alpha_{41}^d = \alpha_{41}.$
Variant types	v_{r9}	v_{r10}
Types of the four spherical 4R linkages	$\alpha_{12}^a = \alpha_{12}, \alpha_{12}^b = \alpha_{12}, \alpha_{12}^c = \pi - \alpha_{12}, \alpha_{12}^d = \alpha_{12},$ $\alpha_{23}^a = \pi - \alpha_{23}, \alpha_{23}^b = \pi - \alpha_{23}, \alpha_{23}^c = \pi - \alpha_{23}, \alpha_{23}^d = \alpha_{23},$ $\alpha_{34}^a = \pi - \alpha_{34}, \alpha_{34}^b = \pi - \alpha_{34}, \alpha_{34}^c = \pi - \alpha_{34}, \alpha_{34}^d = \alpha_{34},$ $\alpha_{41}^a = \alpha_{41}, \alpha_{41}^b = \alpha_{41}, \alpha_{41}^c = \pi - \alpha_{41}, \alpha_{41}^d = \alpha_{41}.$	$\alpha_{12}^a = \pi - \alpha_{12}, \alpha_{12}^b = \alpha_{12}, \alpha_{12}^c = \alpha_{12}, \alpha_{12}^d = \alpha_{12},$ $\alpha_{23}^a = \pi - \alpha_{23}, \alpha_{23}^b = \alpha_{23}, \alpha_{23}^c = \alpha_{23}, \alpha_{23}^d = \alpha_{23},$ $\alpha_{34}^a = \pi - \alpha_{34}, \alpha_{34}^b = \pi - \alpha_{34}, \alpha_{34}^c = \pi - \alpha_{34}, \alpha_{34}^d = \alpha_{34},$ $\alpha_{41}^a = \pi - \alpha_{41}, \alpha_{41}^b = \pi - \alpha_{41}, \alpha_{41}^c = \pi - \alpha_{41}, \alpha_{41}^d = \alpha_{41}.$
Variant types	v_{r11}	v_{r12}
Types of the four spherical 4R linkages	$\alpha_{12}^a = \pi - \alpha_{12}, \alpha_{12}^b = \pi - \alpha_{12}, \alpha_{12}^c = \pi - \alpha_{12}, \alpha_{12}^d = \alpha_{12},$ $\alpha_{23}^a = \pi - \alpha_{23}, \alpha_{23}^b = \pi - \alpha_{23}, \alpha_{23}^c = \pi - \alpha_{23}, \alpha_{23}^d = \alpha_{23},$ $\alpha_{34}^a = \pi - \alpha_{34}, \alpha_{34}^b = \alpha_{34}, \alpha_{34}^c = \alpha_{34}, \alpha_{34}^d = \alpha_{34},$ $\alpha_{41}^a = \pi - \alpha_{41}, \alpha_{41}^b = \alpha_{41}, \alpha_{41}^c = \alpha_{41}, \alpha_{41}^d = \alpha_{41}.$	$\alpha_{12}^a = \pi - \alpha_{12}, \alpha_{12}^b = \alpha_{12}, \alpha_{12}^c = \pi - \alpha_{12}, \alpha_{12}^d = \alpha_{12},$ $\alpha_{23}^a = \pi - \alpha_{23}, \alpha_{23}^b = \alpha_{23}, \alpha_{23}^c = \pi - \alpha_{23}, \alpha_{23}^d = \alpha_{23},$ $\alpha_{34}^a = \pi - \alpha_{34}, \alpha_{34}^b = \alpha_{34}, \alpha_{34}^c = \pi - \alpha_{34}, \alpha_{34}^d = \alpha_{34},$ $\alpha_{41}^a = \pi - \alpha_{41}, \alpha_{41}^b = \alpha_{41}, \alpha_{41}^c = \pi - \alpha_{41}, \alpha_{41}^d = \alpha_{41}.$

Table A3 (1) Flat-deployable origami patterns obtained from the variations of double-plane symmetric case ($\alpha_{i(i+1)} \in (0, \pi)$)

Variant types	Additional relationships besides Tab. A2	Origami patterns	Types of the patterns
v_{t1}	$\alpha_{12}+\alpha_{41}=\alpha_{23}+\alpha_{34}=\pi.$	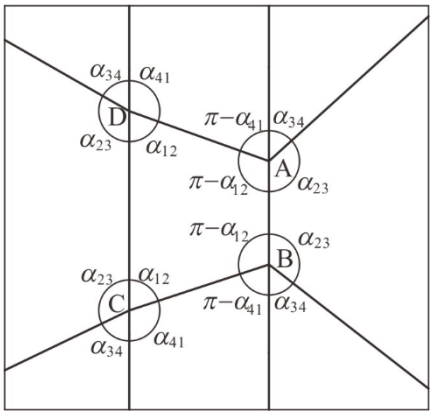	Planar symmetric type
v_{t2}	$\alpha_{12}=\alpha_{41}=\frac{\pi}{2},$ $\alpha_{23}+\alpha_{34}=\pi.$	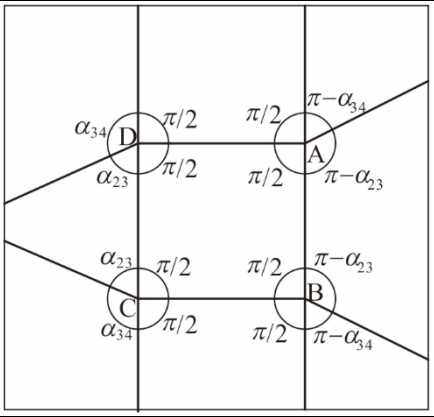	Planar symmetric type
v_{t3}	$\alpha_{12}+\alpha_{23}+\alpha_{34}+\alpha_{41}=2\pi.$	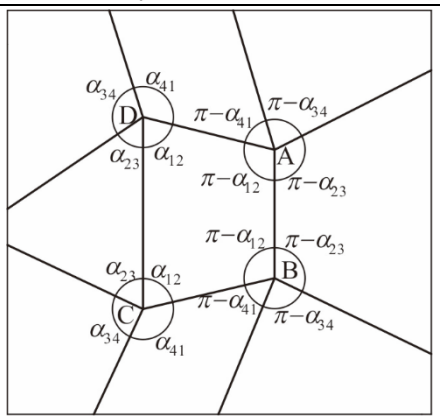	Planar symmetric type

v_{t4}	$\alpha_{12}=\alpha_{23}=\frac{\pi}{2},$ $\alpha_{34}+\alpha_{41}=\pi.$	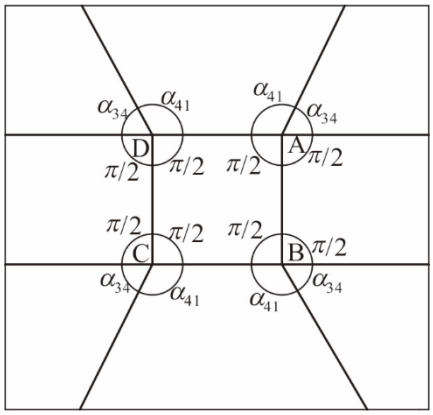	Planar symmetric type
v_{t6}	$\alpha_{12}=\alpha_{23}=\frac{\pi}{2},$ $\alpha_{34}+\alpha_{41}=\pi.$	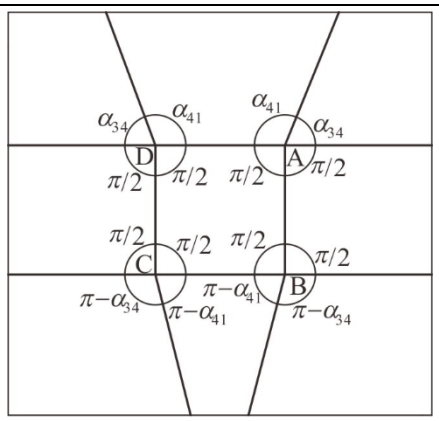	Planar symmetric type
v_{t11}	$\alpha_{12}+\alpha_{41}=\alpha_{23}+\alpha_{34}=\pi.$	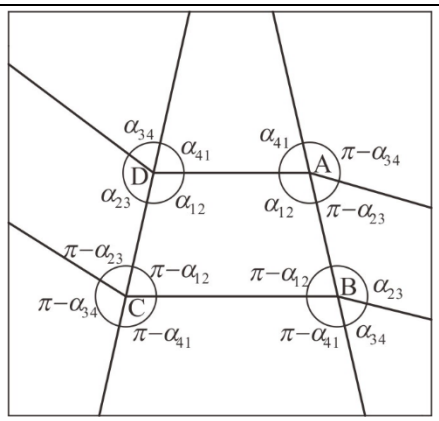	Supplementary type
v_{t13}	$\alpha_{12}+\alpha_{23}=\alpha_{34}+\alpha_{41}=\pi.$	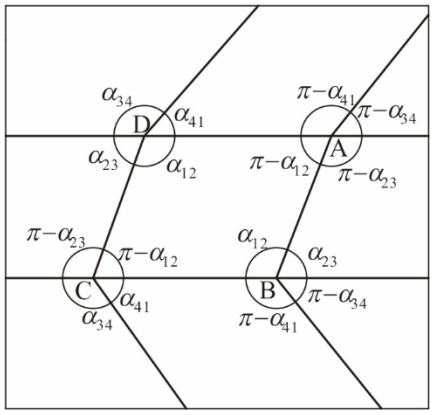	Translational type

v_{t14}	$\alpha_{12}+\alpha_{23}+\alpha_{34}+\alpha_{41}=2\pi.$	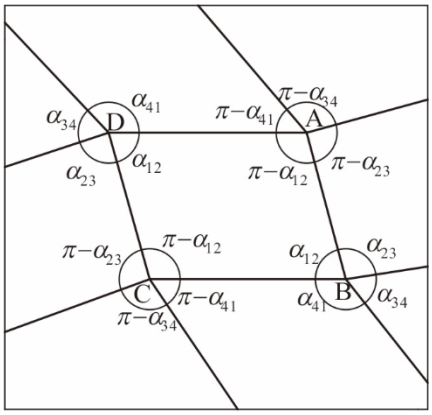	Supplementary type
v_{t15}	$\alpha_{12}+\alpha_{23}=\alpha_{34}+\alpha_{41}=\pi.$	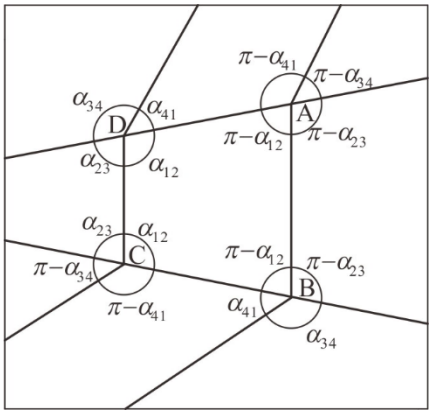	Supplementary type

Table A3 (2) Flat-deployable origami patterns obtained from the variations of plane symmetric case ($\alpha_{i(i+1)} \in (0, \pi)$)

Variant types	Additional relationships besides Tab. A2	Origami patterns	Types of the patterns
v_{s1}	$\alpha_{12} = \alpha_{23} = \frac{\pi}{2}$, $\alpha_{34} + \alpha_{41} = \pi$.	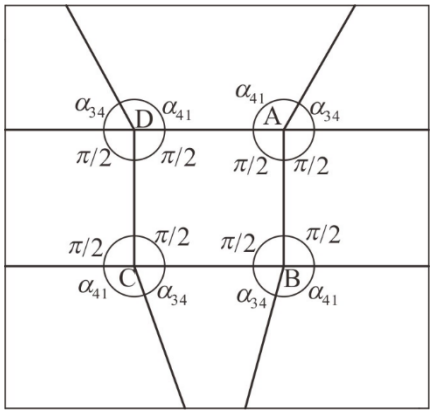	Planar symmetric type
v_{s2}	$\alpha_{12} + \alpha_{23} = \alpha_{34} + \alpha_{41} = \pi$.	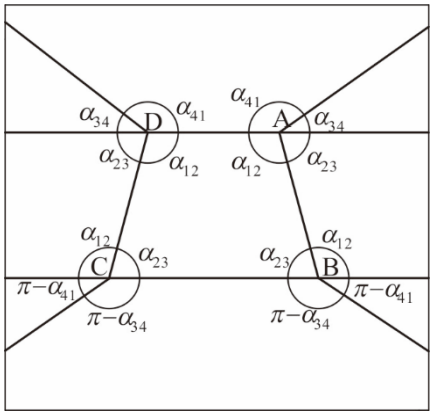	Planar symmetric type
v_{s3}	$\alpha_{12} = \alpha_{23} = \frac{\pi}{2}$, $\alpha_{34} + \alpha_{41} = \pi$.	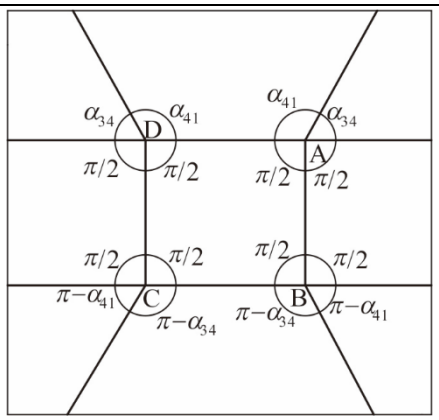	Planar symmetric type

v_{s4}	$\alpha_{12}+\alpha_{41}=\alpha_{23}+\alpha_{34}=\pi.$	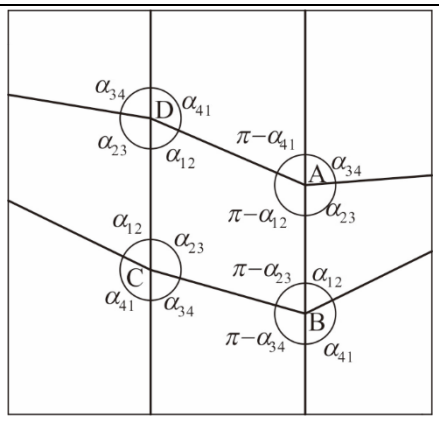	Translational type
v_{s6}	$\alpha_{12}+\alpha_{23}+\alpha_{34}+\alpha_{41}=2\pi.$	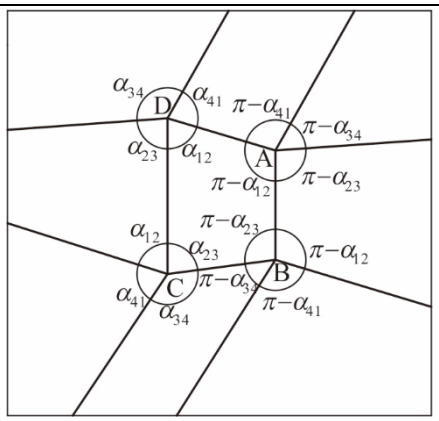	Translational type
v_{s9}	$\alpha_{12}+\alpha_{41}=\alpha_{23}+\alpha_{34}=\pi.$	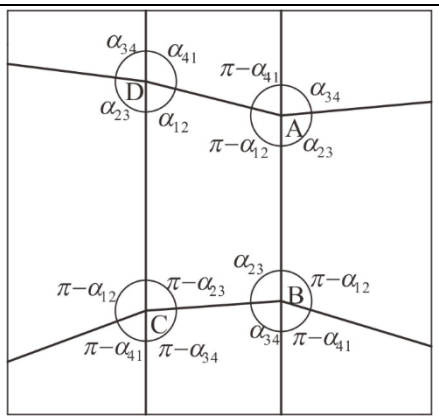	Translational type
v_{s13}	$\alpha_{12}+\alpha_{23}=\alpha_{34}+\alpha_{41}=\pi.$	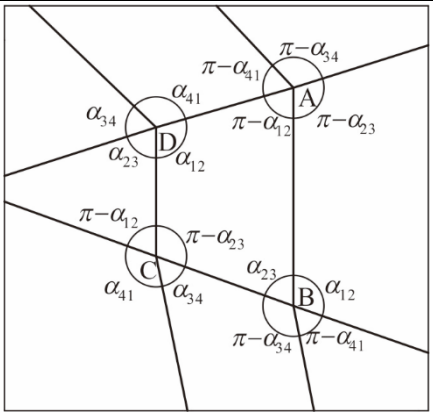	Supplementary type

v_{S14}	$\alpha_{12}+\alpha_{23}=\alpha_{34}+\alpha_{41}=\pi.$	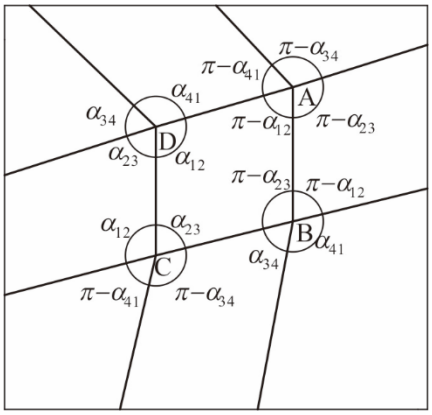	Supplementary type
v_{S15}	$\alpha_{12}+\alpha_{23}+\alpha_{34}+\alpha_{41}=2\pi.$	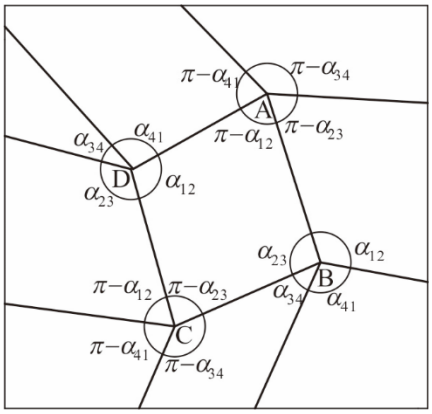	Supplementary type

Table A3 (3) Flat-deployable origami patterns obtained from the variations of rotational case ($\alpha_{i(i+1)} \in (0, \pi)$)

Variant types	Additional relationships besides Tab. A2	Origami patterns	Types of the patterns
v_{r2}	$\alpha_{12}+\alpha_{41}=\alpha_{23}+\alpha_{34}=\pi.$	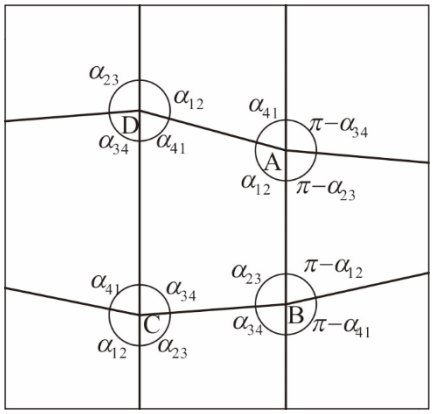	Translational type
v_{r3}	$\alpha_{12}+\alpha_{23}=\alpha_{34}+\alpha_{41}=\pi.$	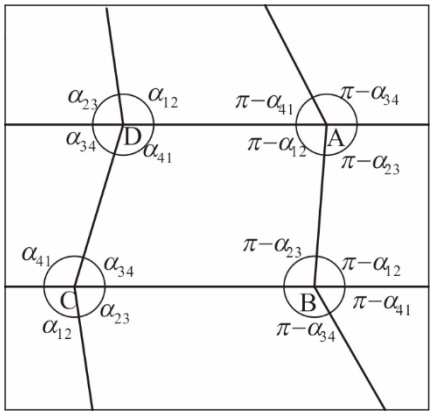	Supplementary type
v_{r7}	$\alpha_{12}+\alpha_{41}=\alpha_{23}+\alpha_{34}=\pi.$	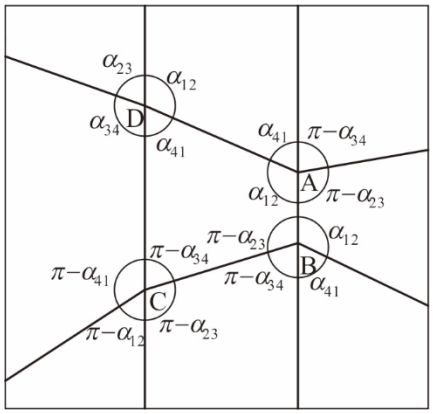	Translational type

v_{r12}	$\alpha_{12}+\alpha_{23}=\alpha_{34}+\alpha_{41}=\pi.$	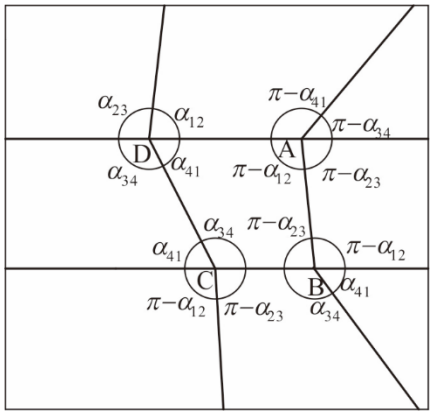	Translational type